First results on the plasma fluctuations of the TORPEX device in the new magnetic field configurations

PhD Thesis: Turbulence at the boundary of toroidal plasmas with open and closed magnetic flux surfaces

F. Avino
A. Bovet, A. Fasoli, I. Furno, J. Loizu, A. Mosetto, P. Ricci

ÉCOLE POLYTECHNIQUE
FÉDÉRALE DE LAUSANNE

2nd PhD Event in Fusion Science and Engineering, October 24, 2012

CRPP

Introduction

- TORPEX
- In-vessel toroidal wire project

Preliminary experimental results

- 1-D plasma profiles (LFS, z=0)
- 2-D plasma profiles

TORoidal Plasma EXperiment[1]

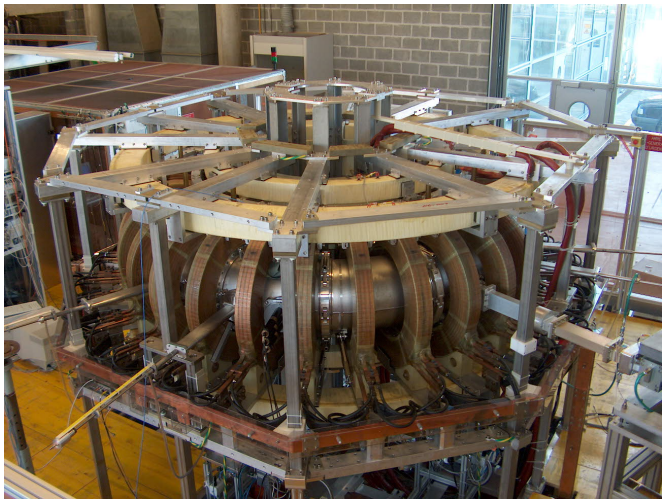

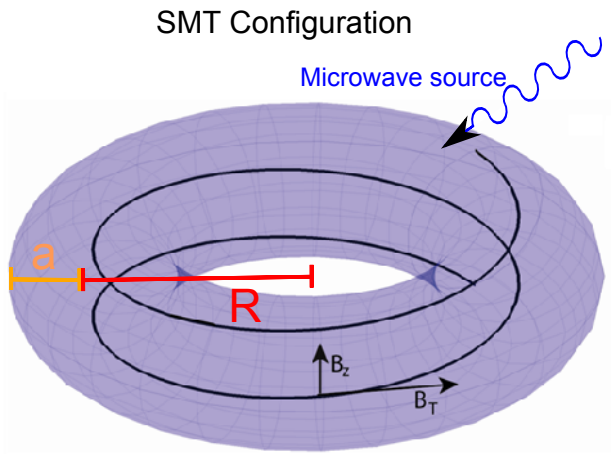

- $R = 1m,\ a = 0.2m$
- H_2, He, Ne, Ar
- $B_T \approx 76mT$
- $B_V \approx mT$
- $n_e \approx 10^{16} m^{-3}$
- $T_e \approx 5eV$

[1] Podestá *et al.* Europhys. Conf. Abstr. vol. 27A, 2003.

TORoidal Plasma EXperiment[1]

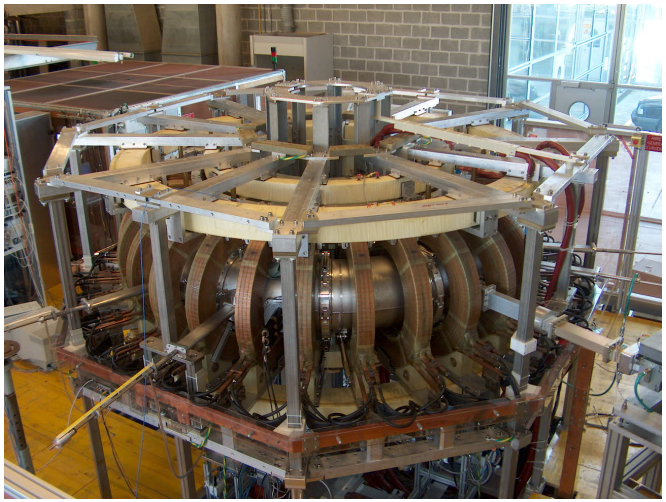

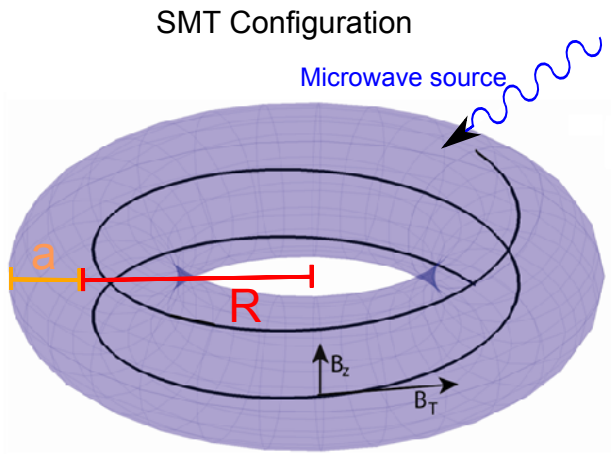

- $R = 1m,\ a = 0.2m$
- H_2, He, Ne, Ar
- $B_T \approx 76mT$
- $B_V \approx mT$
- $n_e \approx 10^{16} m^{-3}$
- $T_e \approx 5eV$

Features :

- Density gradients ;
- Magnetic field gradient ;
- Magnetic field curvature ;

[1] Podestá *et al.* Europhys. Conf. Abstr. vol. 27A, 2003.

TORoidal Plasma EXperiment[1]

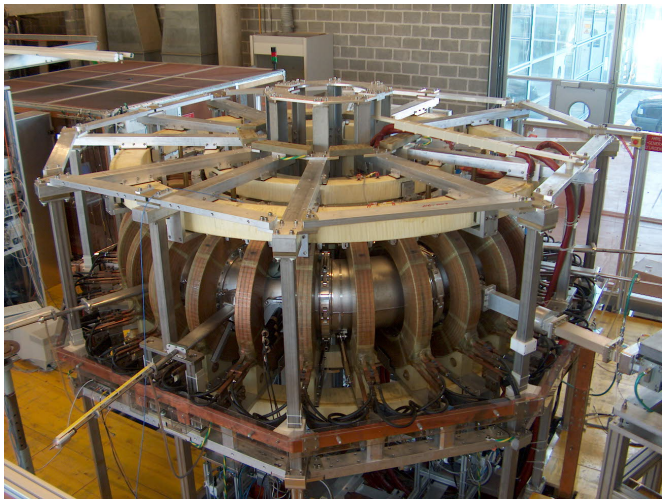

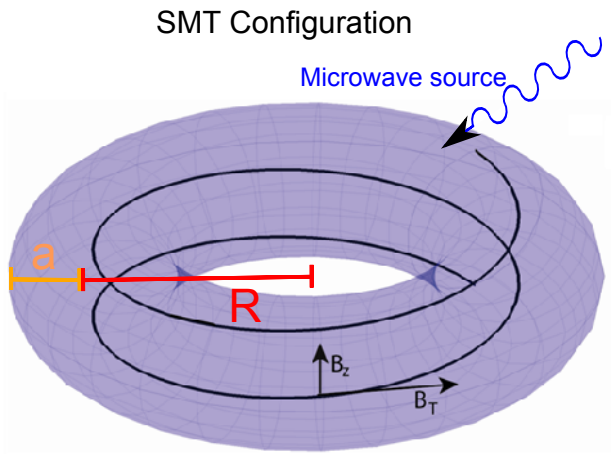

- $R = 1m,\ a = 0.2m$
- H_2, He, Ne, Ar
- $B_T \approx 76mT$
- $B_V \approx mT$
- $n_e \approx 10^{16} m^{-3}$
- $T_e \approx 5eV$

Features :

- Density gradients ;
- Magnetic field gradient ;
- Magnetic field curvature ;

Advantages :

- Direct measurements on the whole plasma volume.
- High plasma reproducibility.
- High flexibility of the control parameters.

[1] Podestá *et al.* Europhys. Conf. Abstr. vol. 27A, 2003.

TORoidal Plasma EXperiment[1]

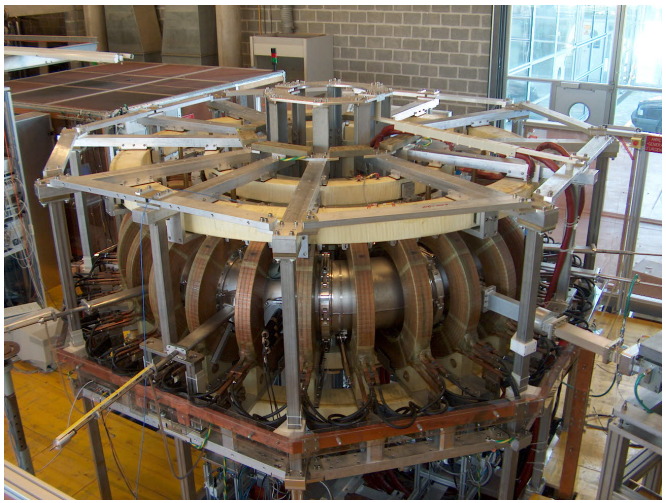

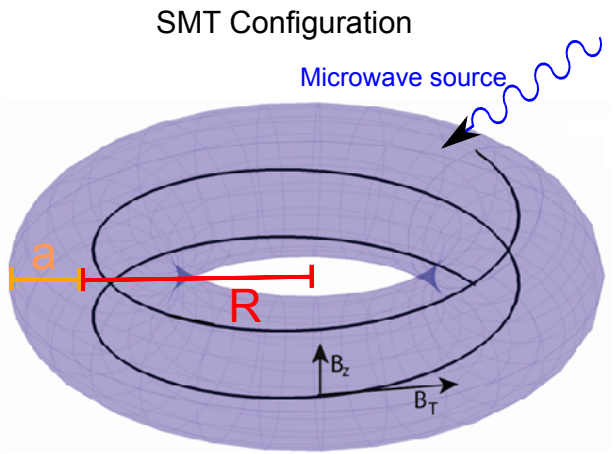

- $R = 1m,\ a = 0.2m$
- H_2, He, Ne, Ar
- $B_T \approx 76mT$
- $B_V \approx mT$
- $n_e \approx 10^{16} m^{-3}$
- $T_e \approx 5eV$

Features :

- Density gradients ;
- Magnetic field gradient ;
- Magnetic field curvature ;

Advantages :

- Direct measurements on the whole plasma volume.
- High plasma reproducibility.
- High flexibility of the control parameters.

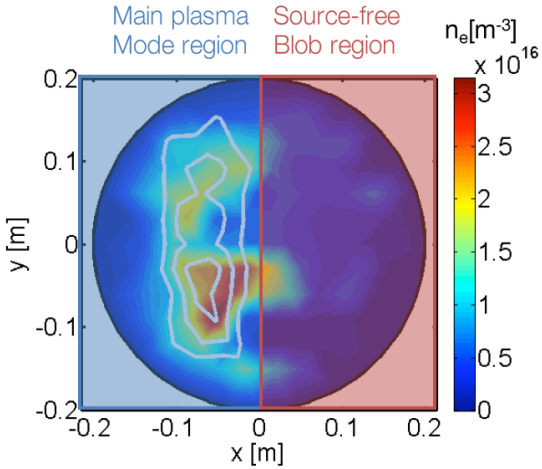

[1] Podestá *et al.* Europhys. Conf. Abstr. vol. 27A, 2003.

Example of blob propagation

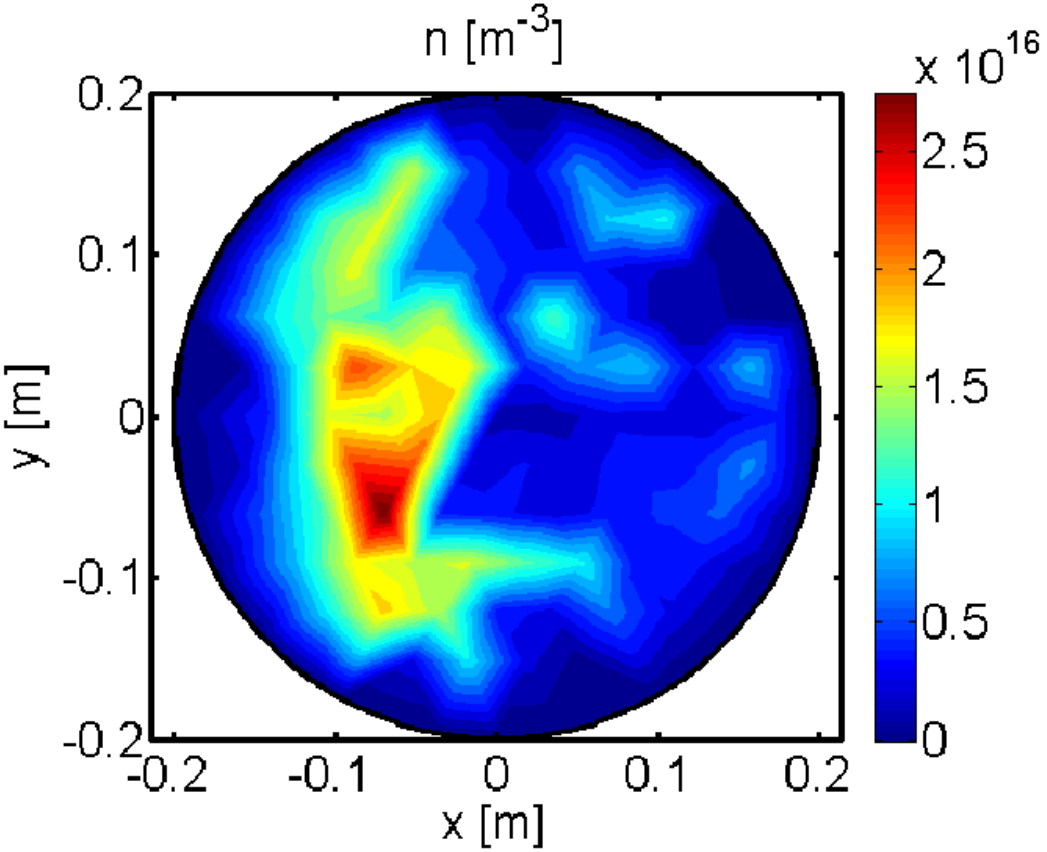

How have we obtained the new magnetic f. configurations ?

SMT Configuration

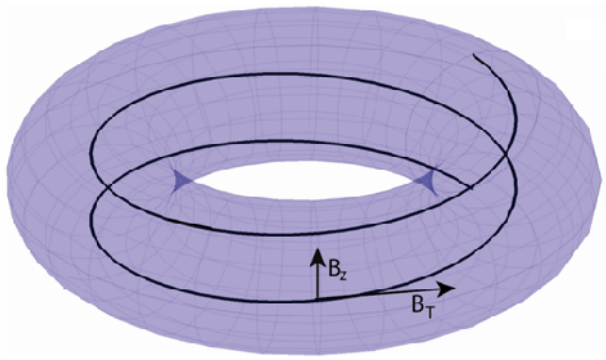

How have we obtained the new magnetic f. configurations ?

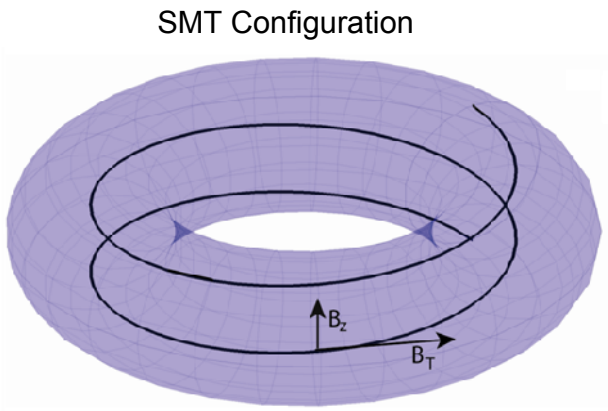

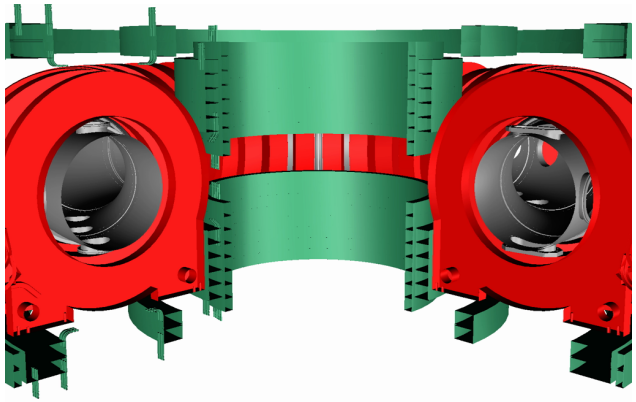

How have we obtained the new magnetic f. configurations ?

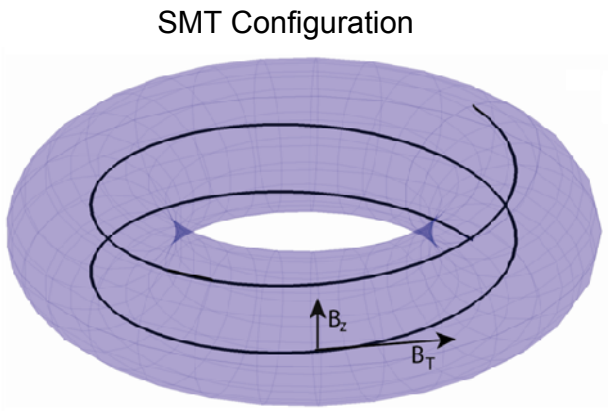

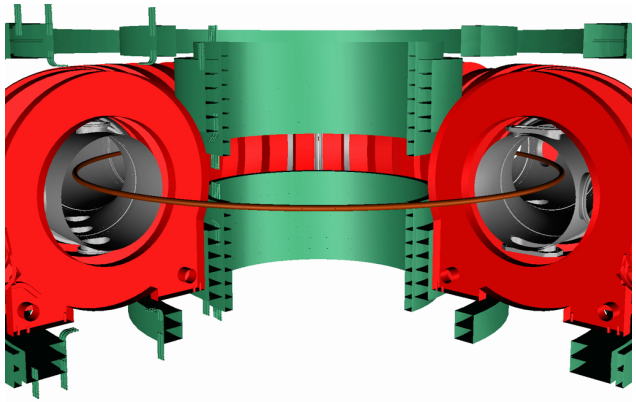

How have we obtained the new magnetic f. configurations ?

SMT Configuration

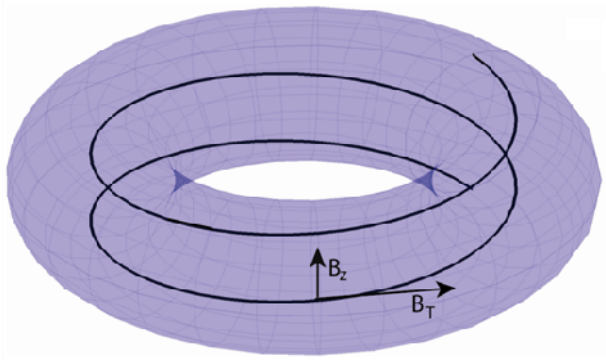

TORPEX configuration with the toroidal wire

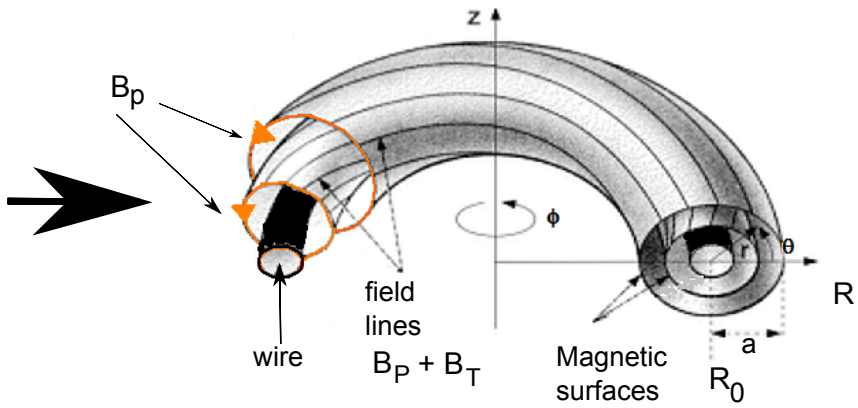

Why ? In-vessel toroidal copper wire ⇒ poloidal field ⇒ rotational transform.

How have we obtained the new magnetic f. configurations ?

SMT Configuration

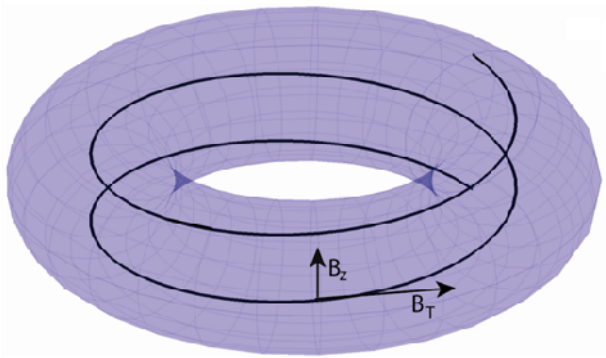

TORPEX configuration with the toroidal wire

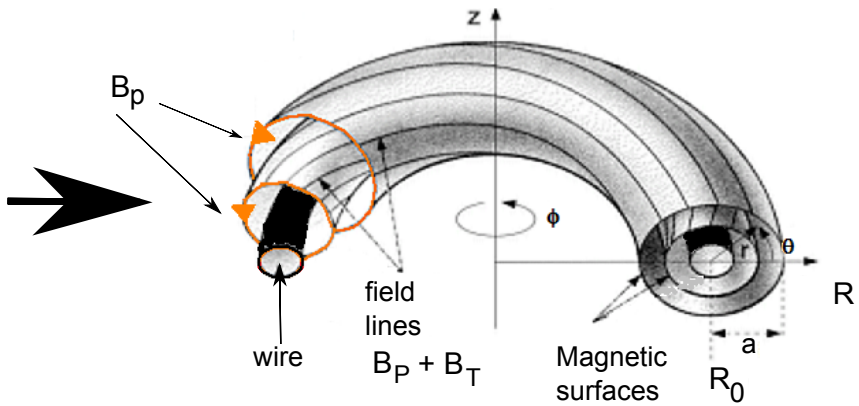

Why ? In-vessel toroidal copper wire ⇒ poloidal field ⇒ rotational transform.

- TORPEX closer to a tokamak configuration.
- Plasma decoupled from the magnetic field source.
- Scrape-Off Layer physics.
- Closed-to-open magnetic surfaces transition.
- Core region.

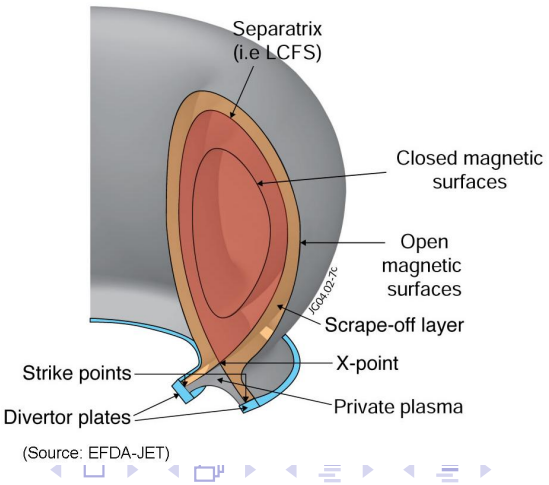

Experimental set-up

- Toroidal copper wire with 1cm radius ;
- 3 vertical supports + 1 vertical feed-through ;
- 4 horizontal supports ;
- up to $1kA$ of current ;

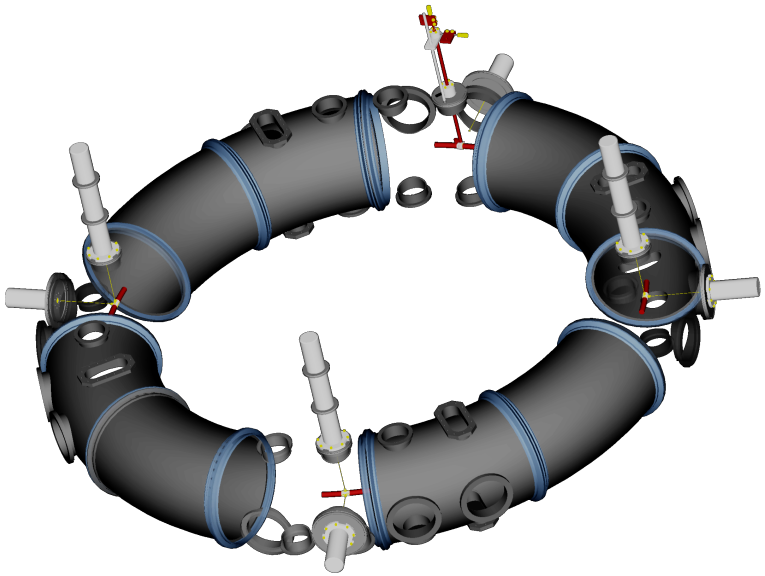

Experimental set-up

- Toroidal copper wire with 1cm radius ;
- 3 vertical supports + 1 vertical feed-through ;
- 4 horizontal supports ;
- up to $1kA$ of current ;

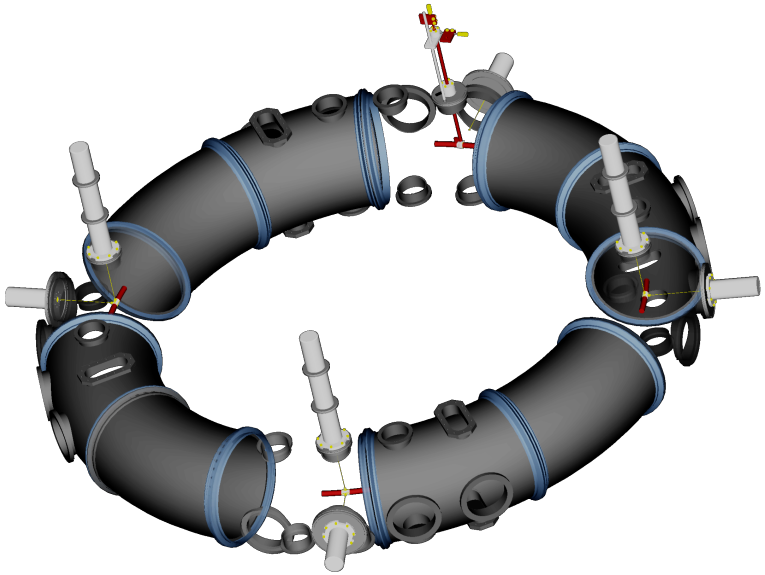

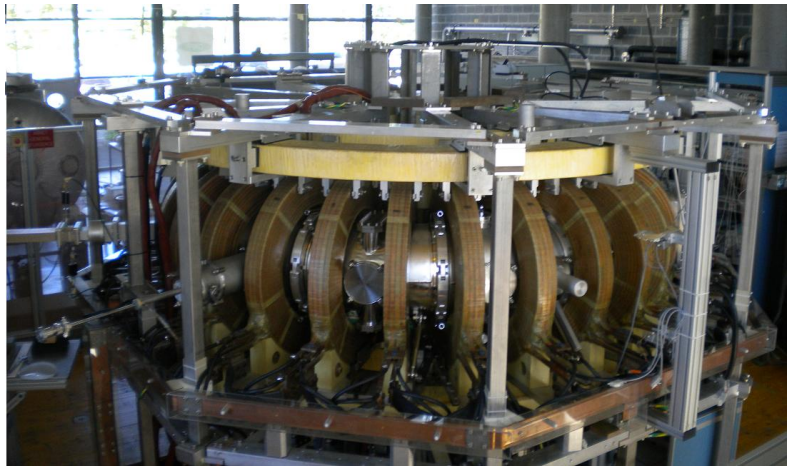

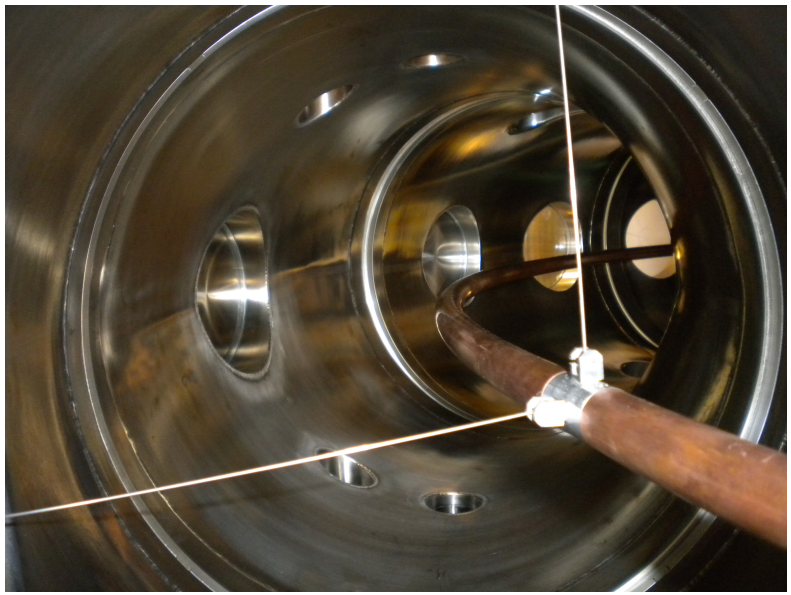

Experimental set-up

- Toroidal copper wire with 1cm radius ;
- 3 vertical supports + 1 vertical feed-through ;
- 4 horizontal supports ;
- up to $1kA$ of current ;

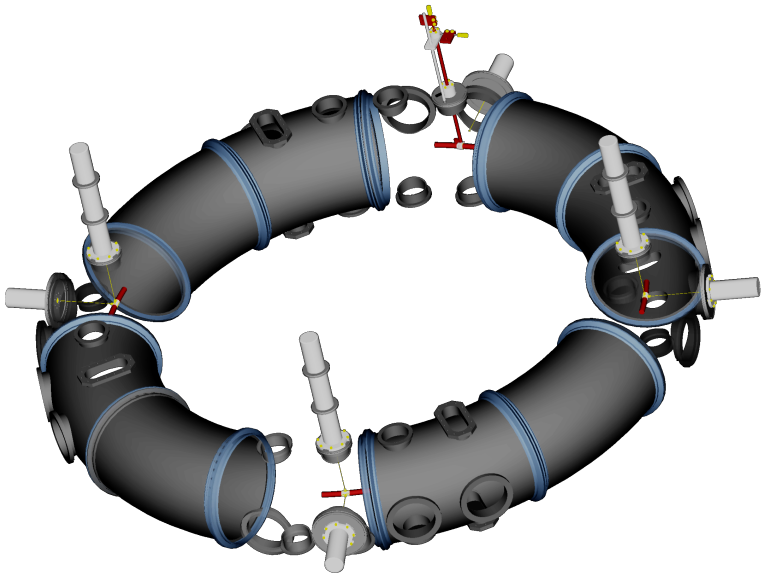

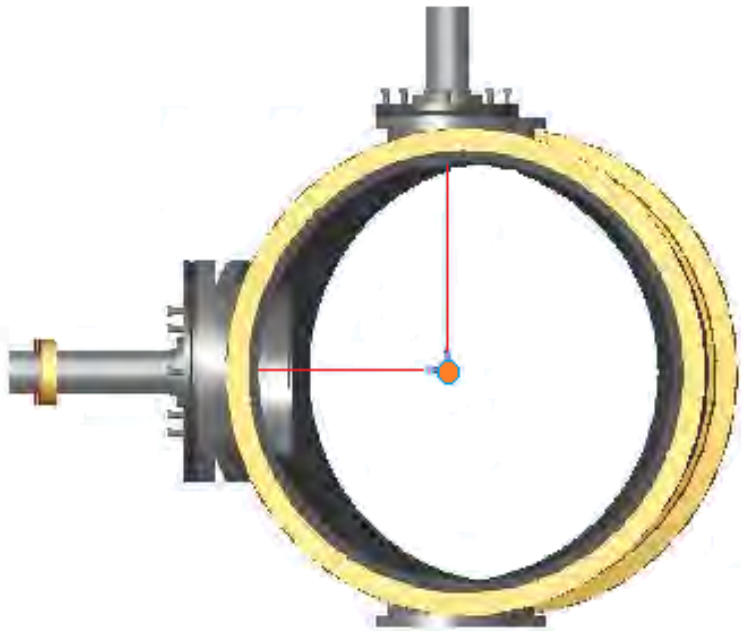

Experimental set-up

- Toroidal copper wire with 1cm radius ;
- 3 vertical supports + 1 vertical feed-through ;
- 4 horizontal supports ;
- up to $1kA$ of current ;

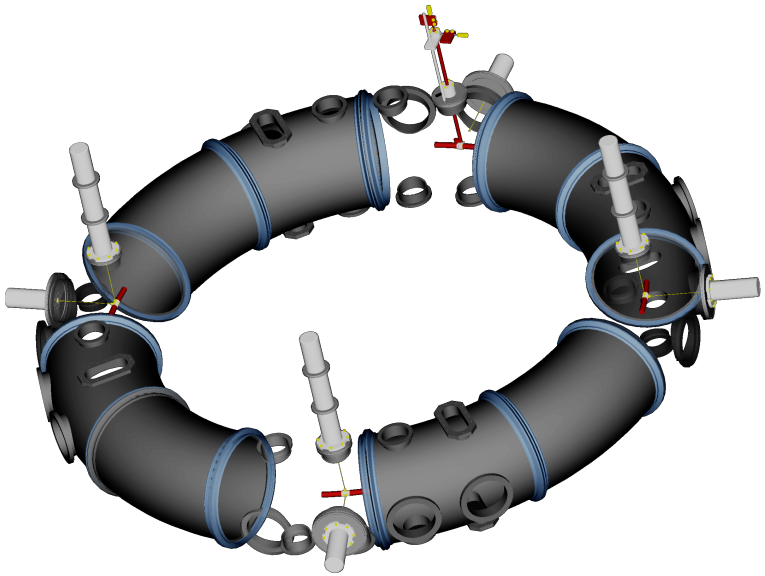

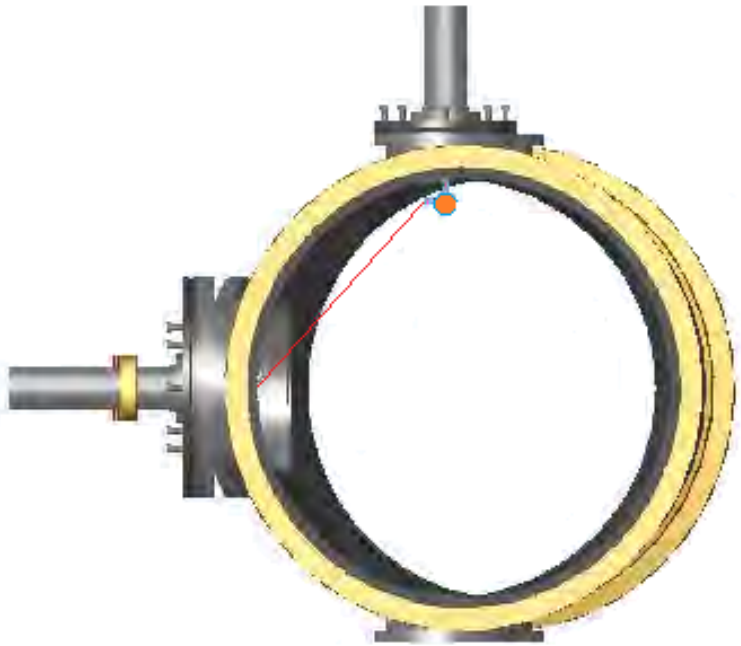

Experimental set-up

- Toroidal copper wire with 1cm radius ;
- 3 vertical supports + 1 vertical feed-through ;
- 4 horizontal supports ;
- up to $1kA$ of current ;

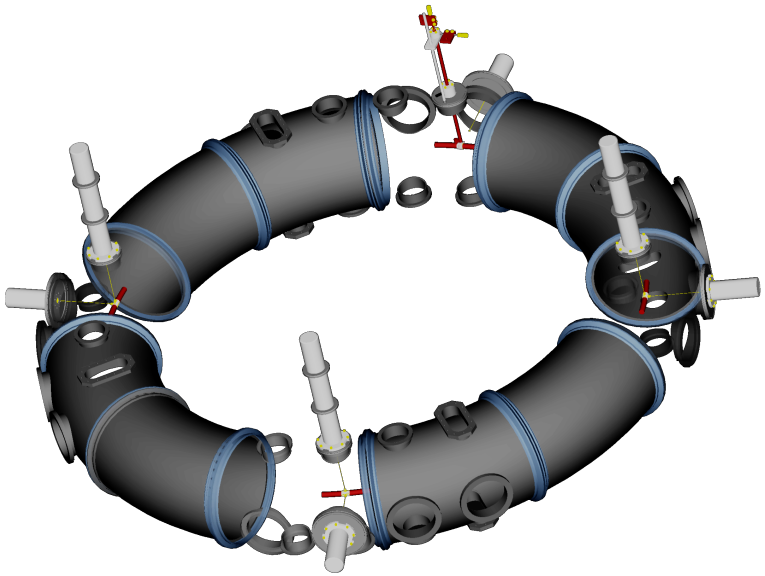

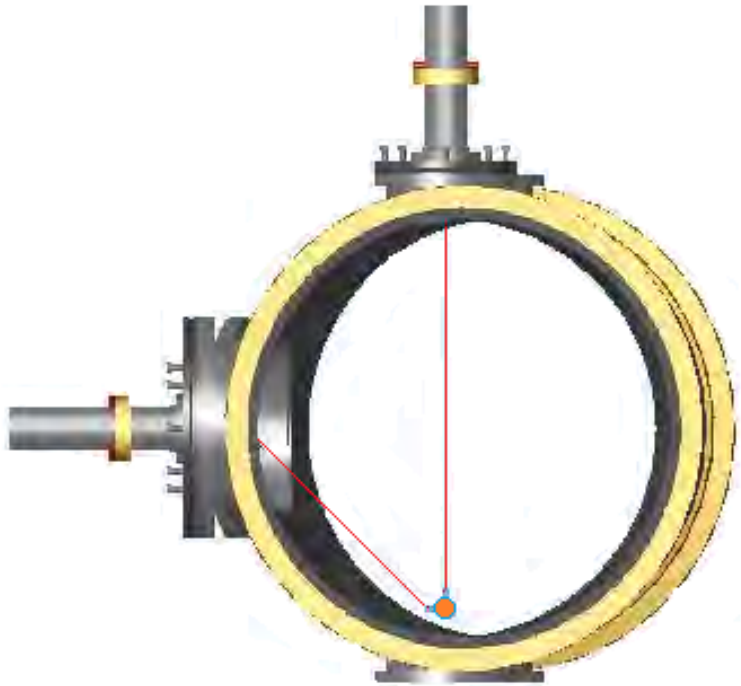

Simulated magnetic field configurations

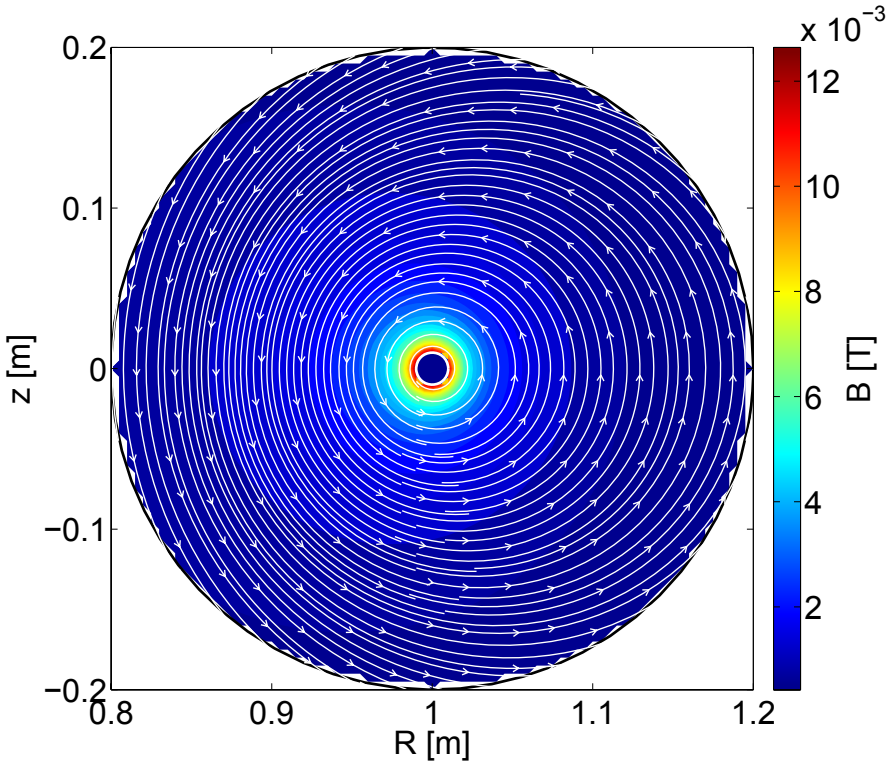

Simulated magnetic field configurations

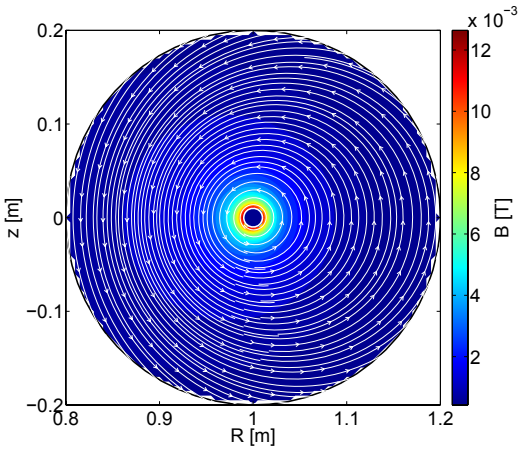

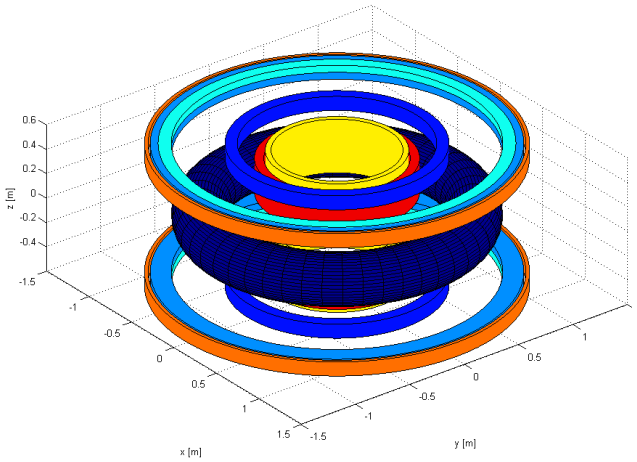

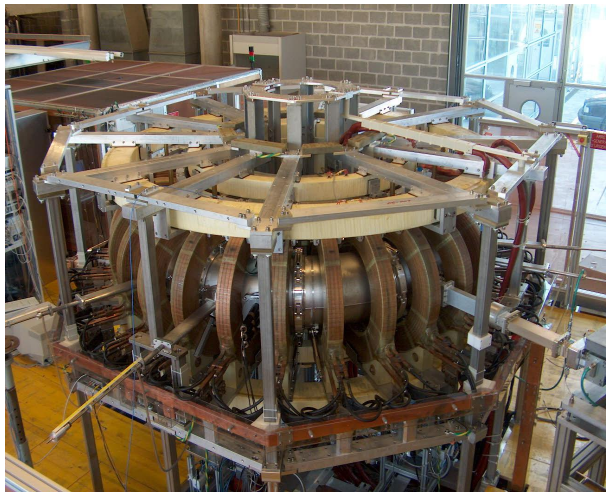

Simulated magnetic field configurations

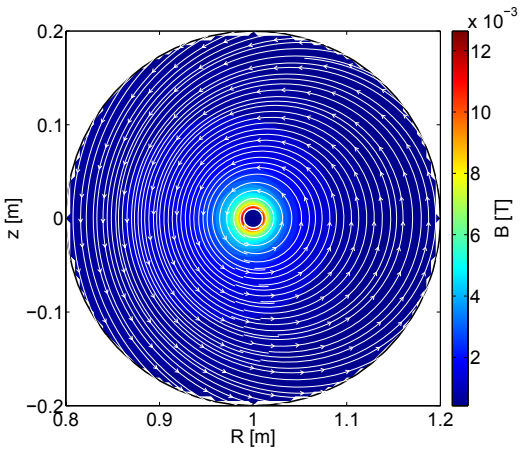

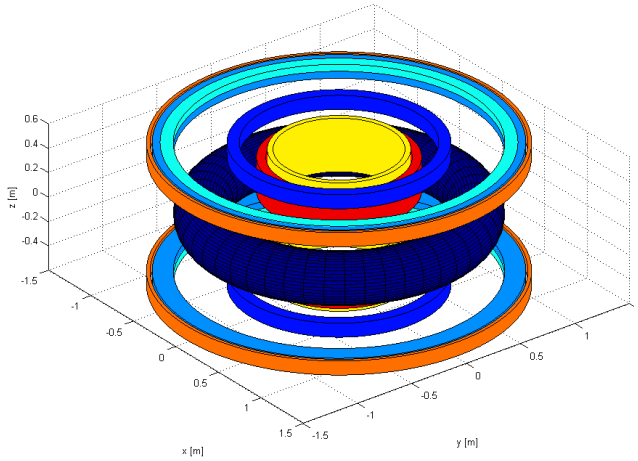

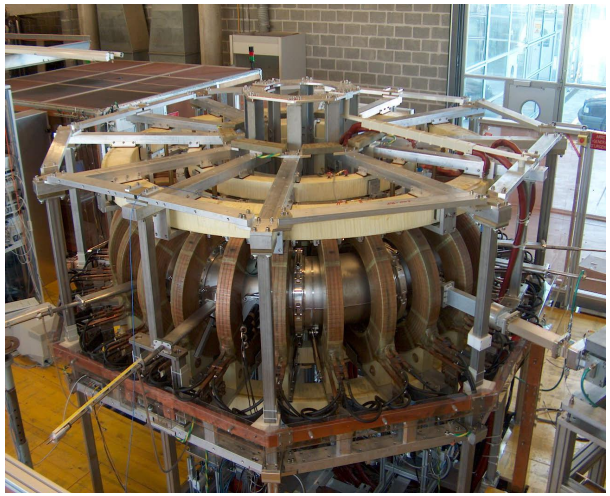

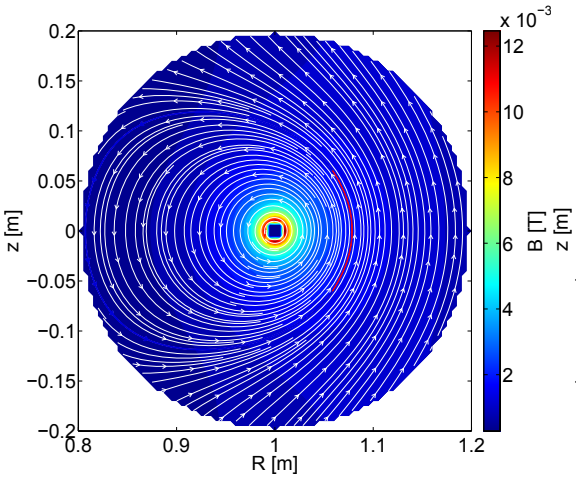

LFS Scrape-off layer

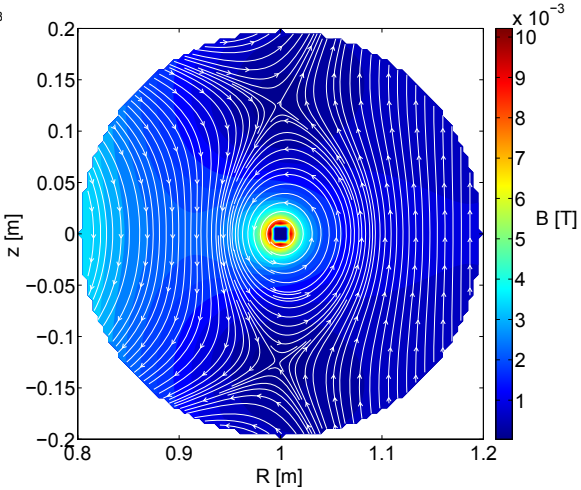

Vertical Double-Null X-points

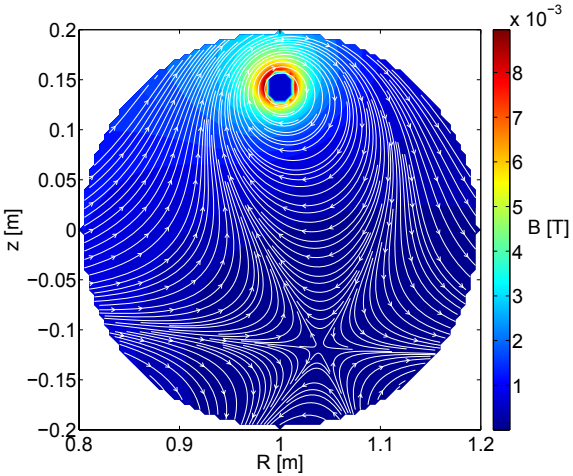

Snowflake

Plasma time-averaged measurements, $R_{EC} = 0.9m$

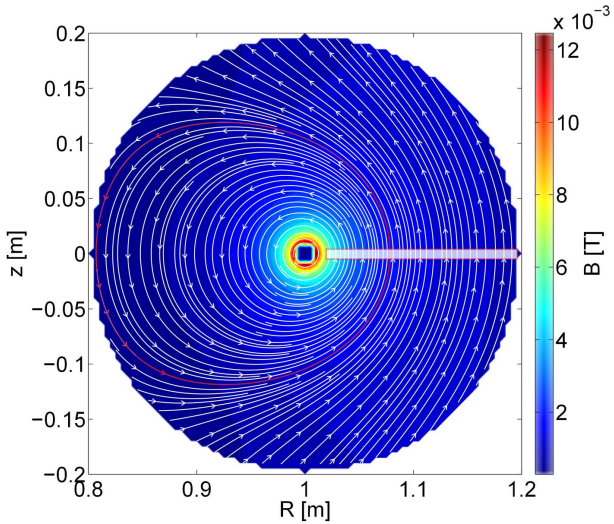

LFS Scrape-off layer

TWIN-1 : one of two identical single pin Langmuir probes.

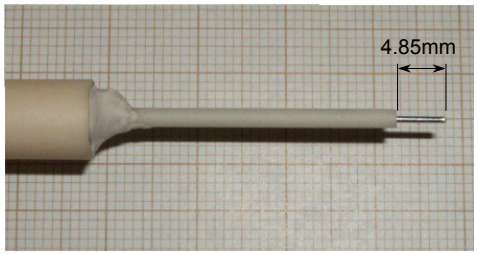

2DSSLP : a 2-D array of 8 Single-Sided Langmuir Probes.

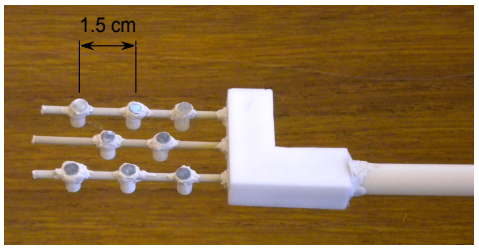

Plasma time-averaged measurements, $R_{EC} = 0.9m$

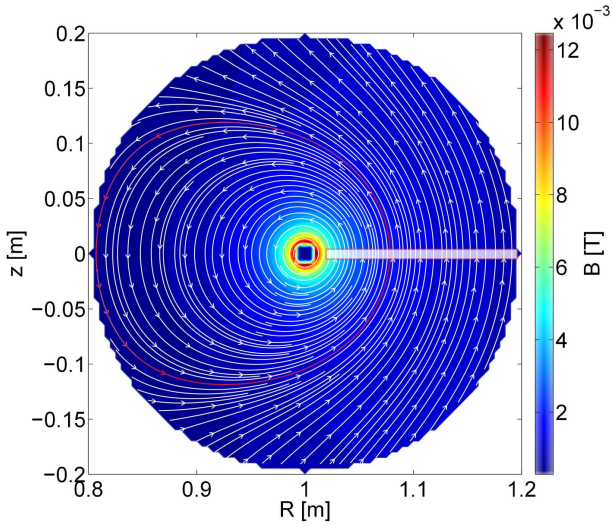

LFS Scrape-off layer

TWIN-1 : one of two identical single pin Langmuir probes.

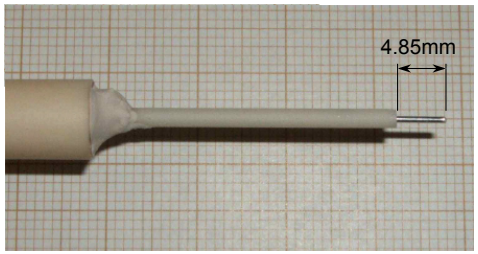

2DSSLP : a 2-D array of 8 Single-Sided Langmuir Probes.

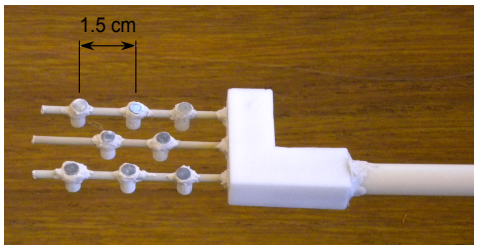

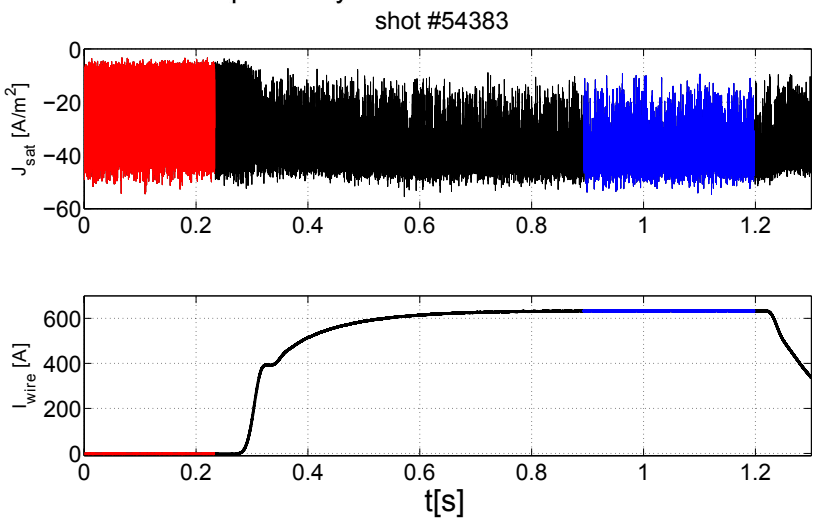

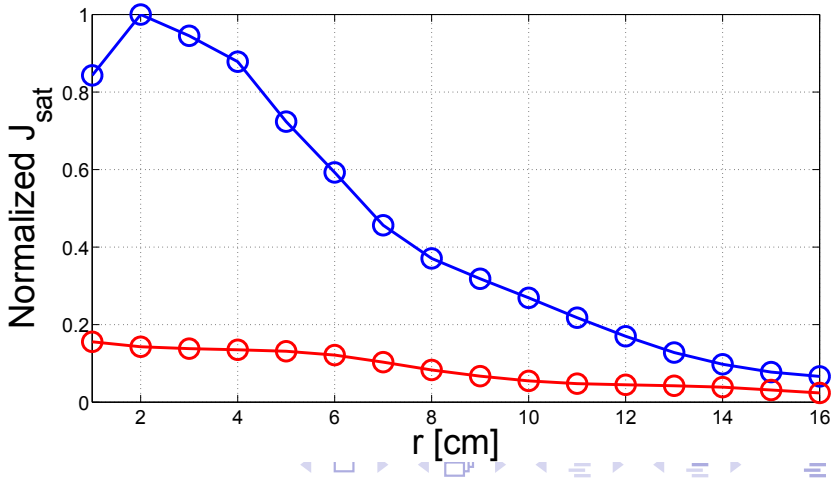

Plasma fluctuations measurements, $R_{EC} = 1.0m$

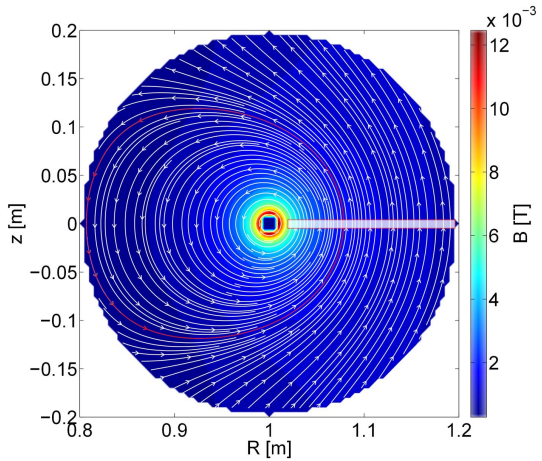

LFS Scrape-off layer

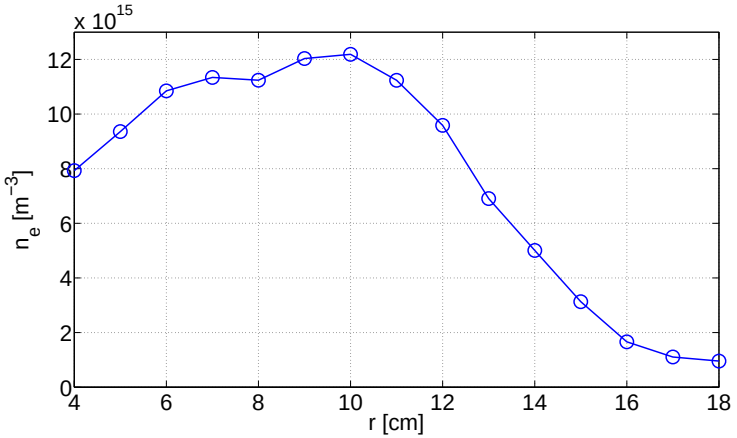

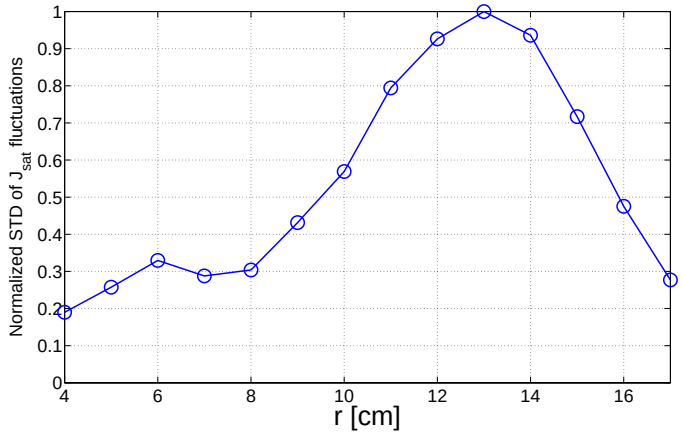

Plasma fluctuations measurements, $R_{EC} = 1.0m$

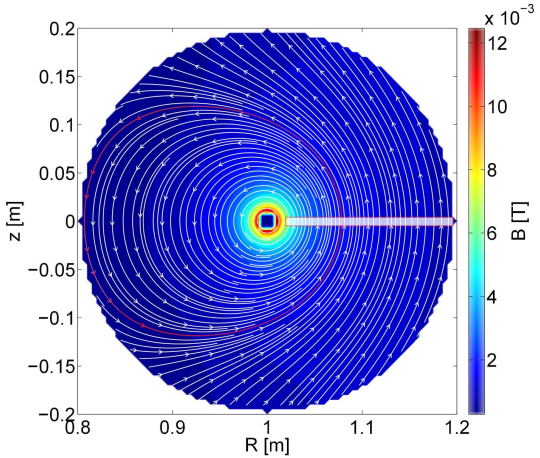

LFS Scrape-off layer

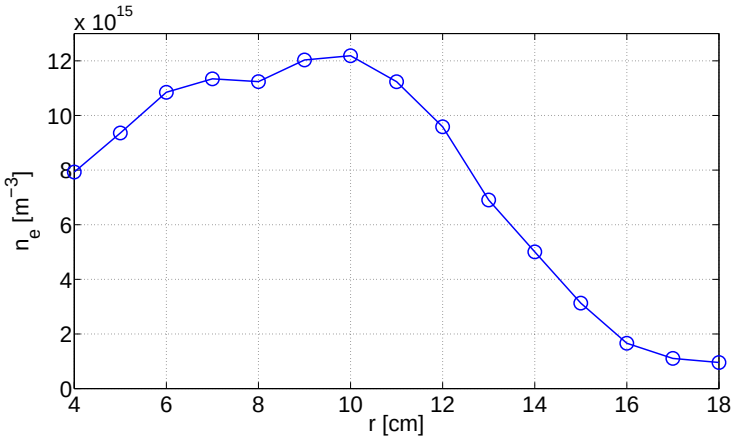

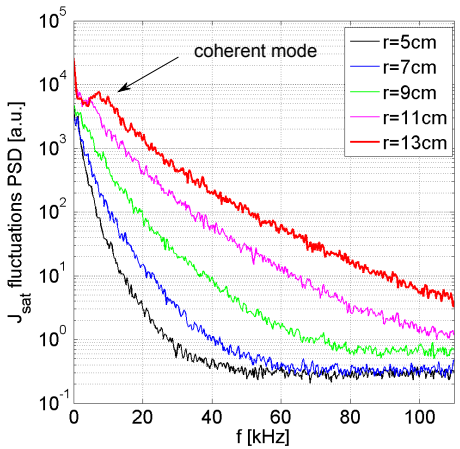

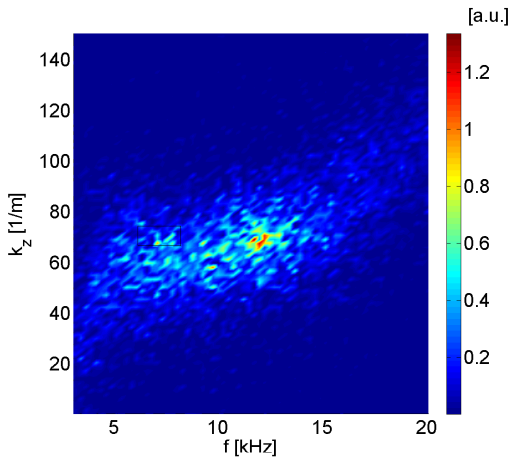

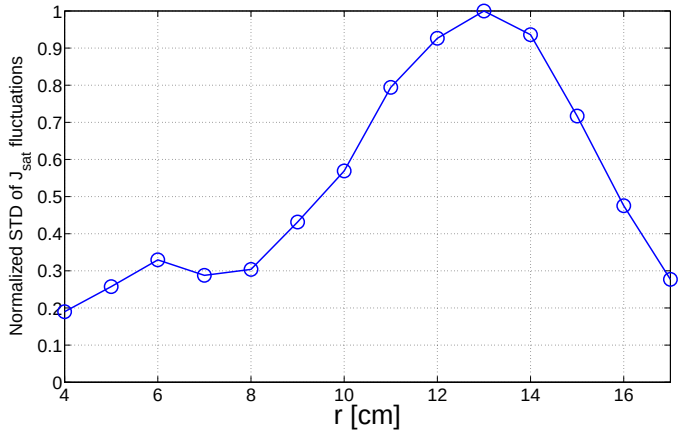

The statistical dispersion relation shows a coherent mode at $f \simeq 12kHz$ and $k_z \simeq 70m^{-1}$.

Plasma time-averaged measurements

HEXagonal Turbulence Imaging Probe (HEXTIP) :
85 Langmuir probes covering the whole poloidal cross section.

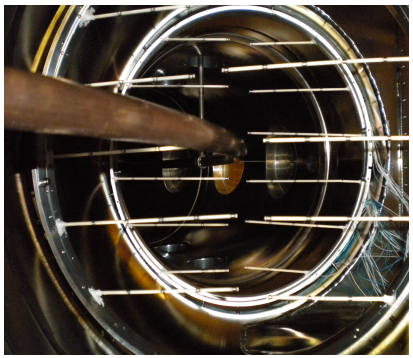

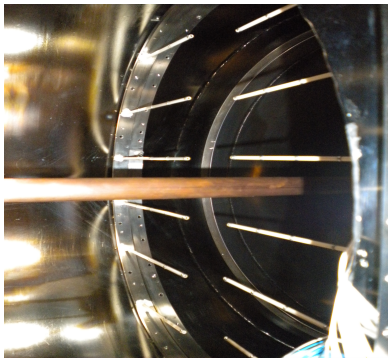

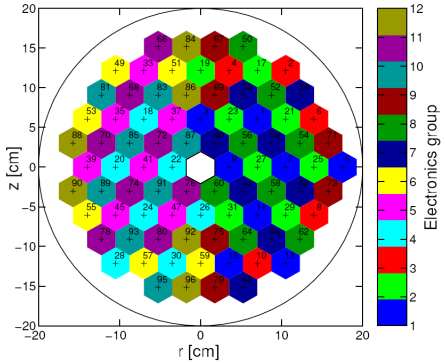

Plasma time-averaged measurements

HEXagonal Turbulence Imaging Probe (HEXTIP) :
85 Langmuir probes covering the whole poloidal cross section.

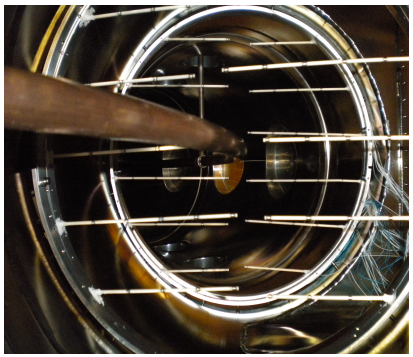

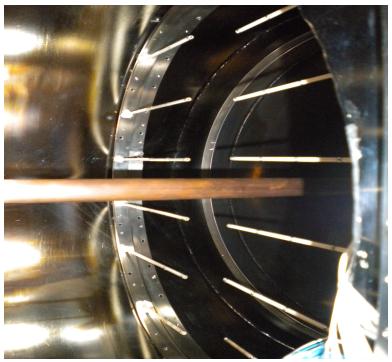

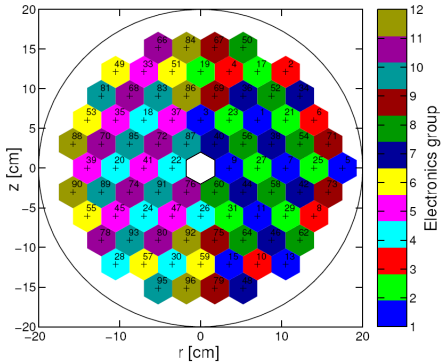

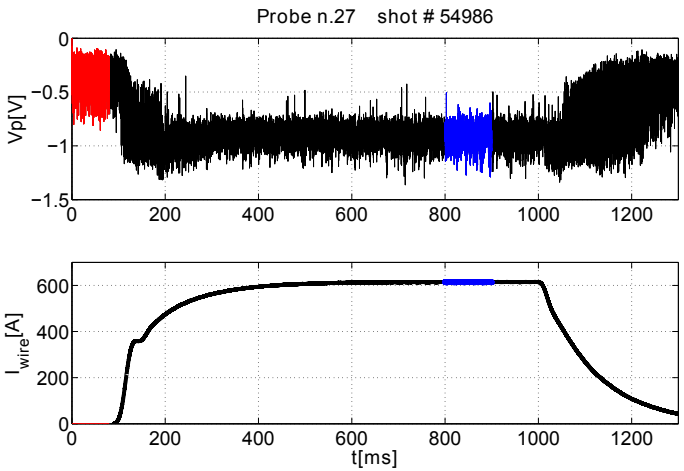

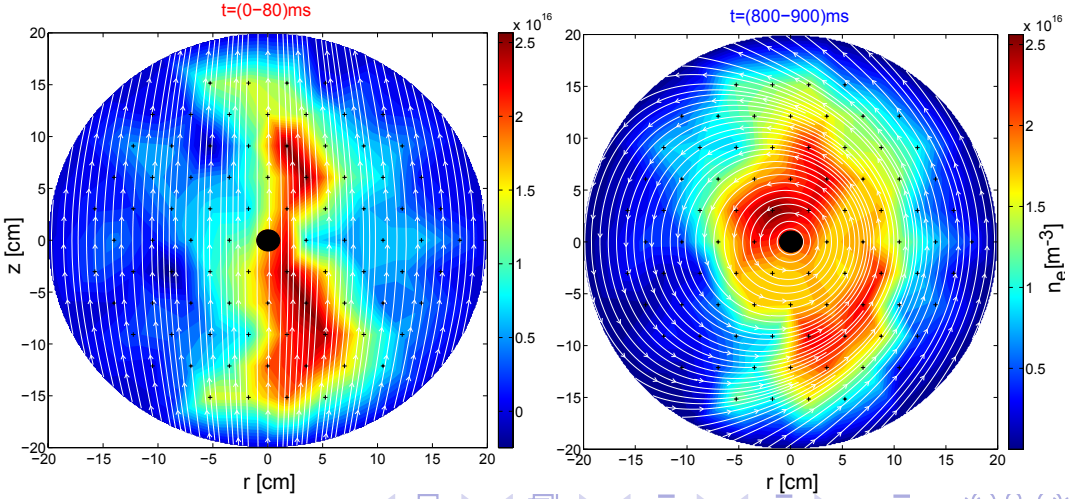

Plasma fluctuations measurements

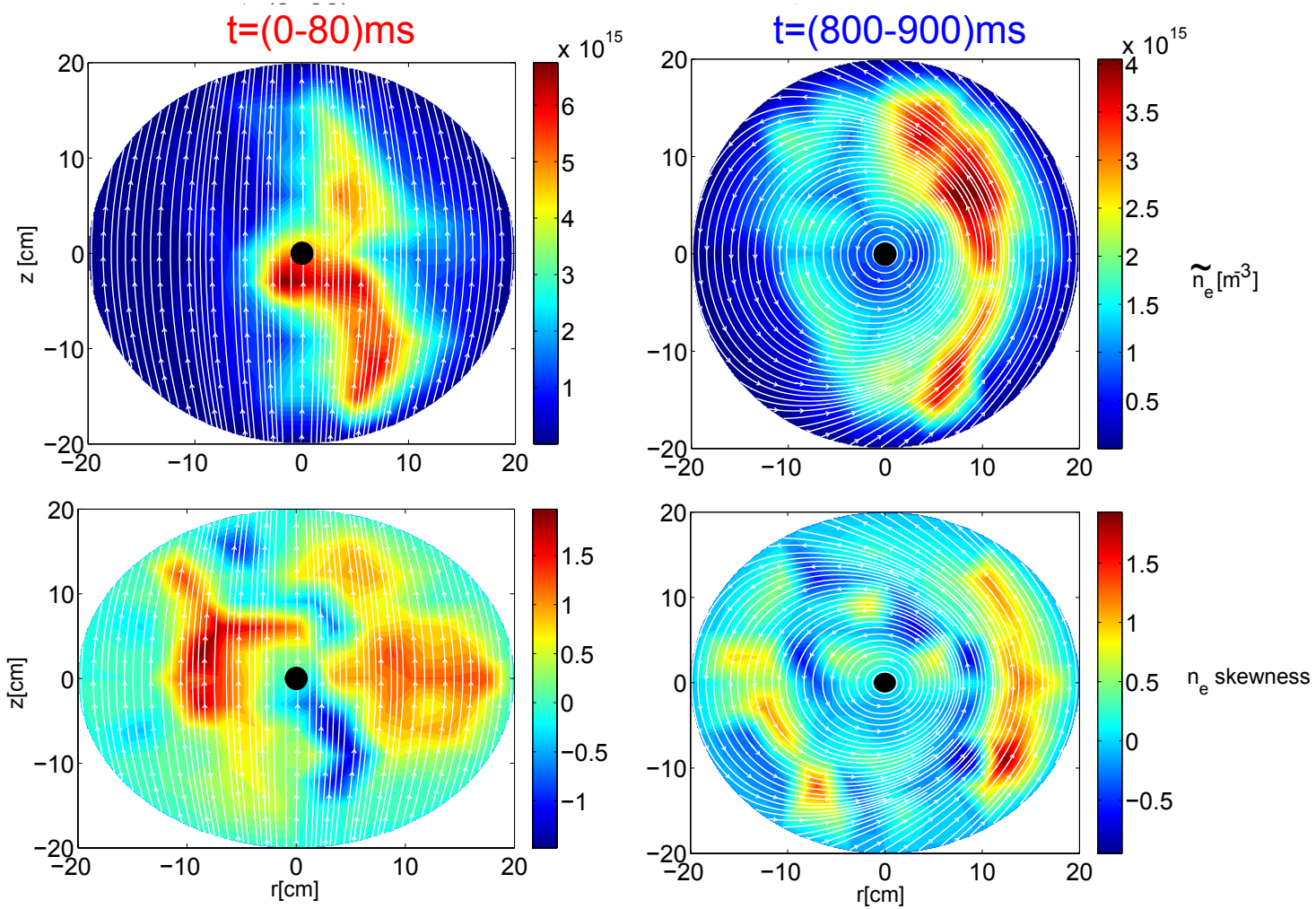

Conditional sampling evolution

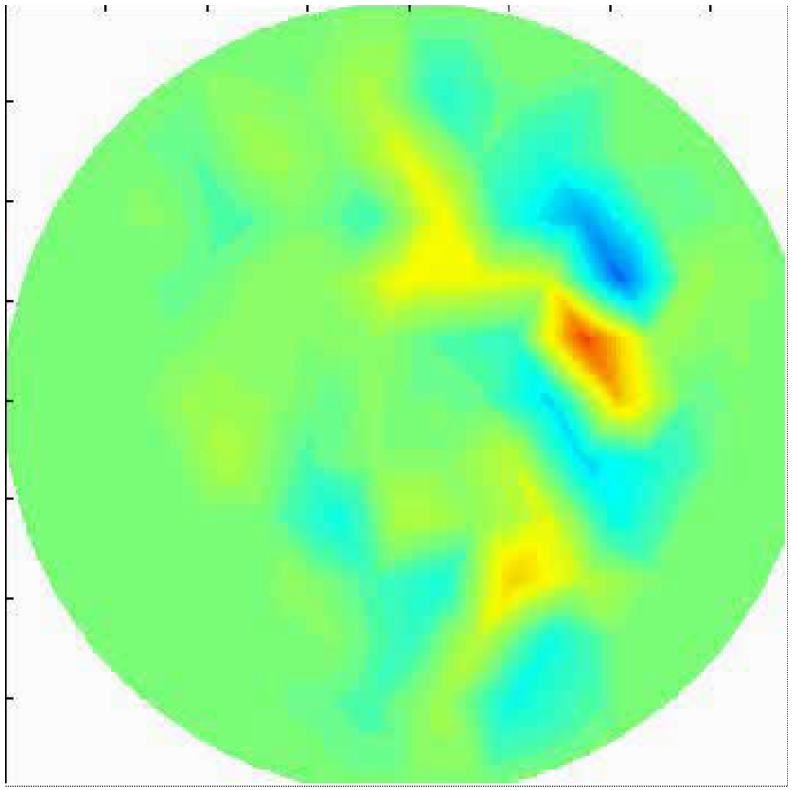

Conclusions

- Introduced the TORPEX in-vessel toroidal wire ;
- Shown the first 1-D experimental results :

$$\begin{cases} \text{time-averaged plasma quantities} \\ \text{plasma fluctuations} \end{cases} \quad (1)$$

- Shown the first 2-D experimental results :

$$\begin{cases} \text{time-averaged plasma quantities} \\ \text{plasma fluctuations} \end{cases} \quad (2)$$

Thanks to my supervisors Dr. Ivo Furno and Prof. Ambrogio Fasoli, the CRPP workshops, Ing. Jürgen Theile and Roger Senn of PSI, and my PhD colleagues.

Conclusions

- Introduced the TORPEX in-vessel toroidal wire ;
- Shown the first 1-D experimental results :

$$\begin{cases} \text{time-averaged plasma quantities} \\ \text{plasma fluctuations} \end{cases} \quad (1)$$

- Shown the first 2-D experimental results :

$$\begin{cases} \text{time-averaged plasma quantities} \\ \text{plasma fluctuations} \end{cases} \quad (2)$$

Thanks to my supervisors Dr. Ivo Furno and Prof. Ambrogio Fasoli, the CRPP workshops, Ing. Jürgen Theile and Roger Senn of PSI, and my PhD colleagues.

THANKS FOR YOUR ATTENTION.

Transport processes

- Particles
- Momentum
- Heat

$\Rightarrow$ Study of plasma turbulence and instabilities

Difficult in tokamak experiment : $T \approx 1keV$, $n_e \approx 10^{20} m^{-3}$.

Transport processes

- Particles
- Momentum
- Heat

$\Rightarrow$ Study of plasma turbulence and instabilities

Difficult in tokamak experiment : $T \approx 1keV$, $n_e \approx 10^{20} m^{-3}$.

- Reciprocating Langmuir probes[1].

[1]

[1] Silva *et al.* Plasma Phys. Control. Fusion, vol. 51 (2009).

Transport processes

- Particles
- Momentum
- Heat

$\Rightarrow$ Study of plasma turbulence and instabilities

Difficult in tokamak experiment : $T \approx 1keV$, $n_e \approx 10^{20} m^{-3}$.

- Reciprocating Langmuir probes[1].
- Fast imaging in the visible range with gas puffing[2].

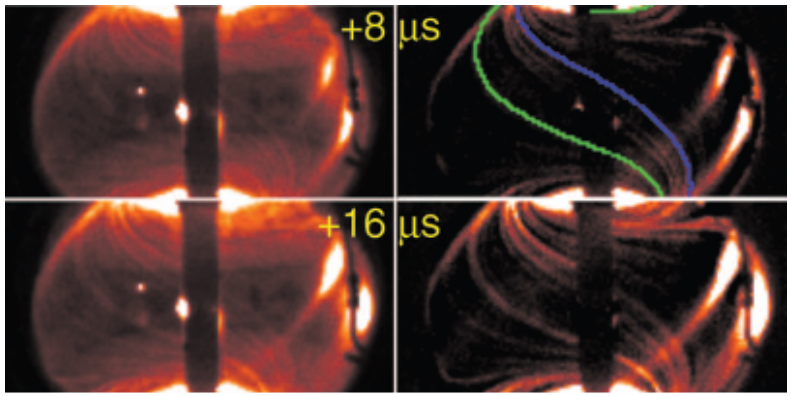

Source: NSTX [2]

[1] Silva *et al.* Plasma Phys. Control. Fusion, vol. 51 (2009).
[2] Maqueda *et al.* Physics of Plasmas, vol. 16 (2009).

TORPEX regimes

Presence of pressure gradients and magnetic field curvature.

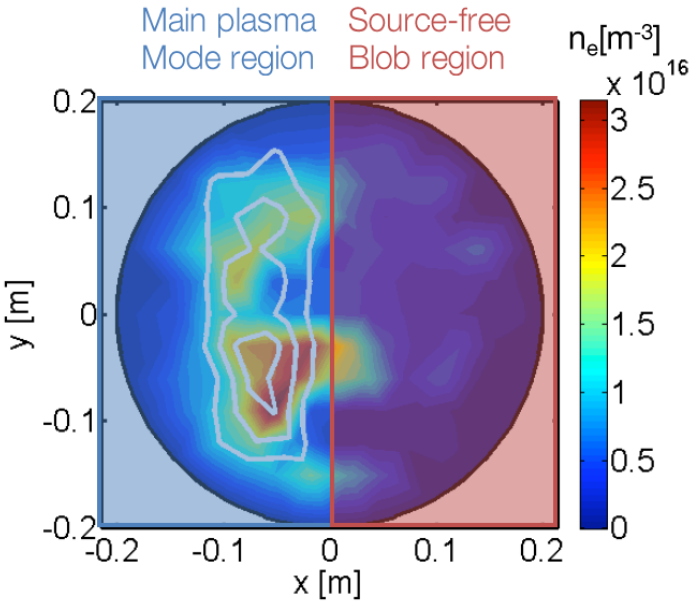

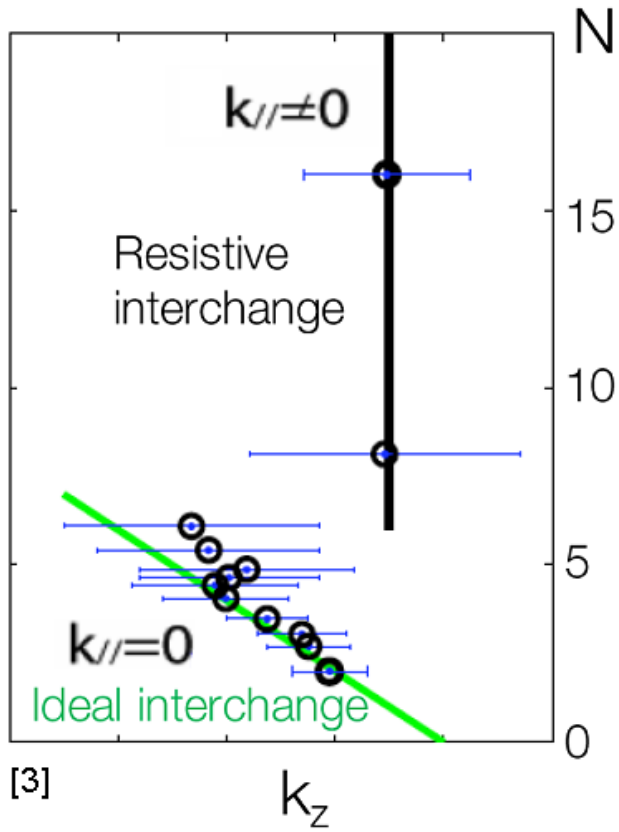

- Electrostatic instabilities, turbulence and fast ions interactions[1].
- Birth, motion and control of plasma blobs[2].

[1] A.Fasoli *et al.* Plasma Phys. Control. Fusion 52 (2010).
[2] C.Theiler *et al.* Phys. Rev. Lett. vol 103, (2009).
[3] P.Ricci *et al.* Phys. Rev. Lett. vol 104, (2010).

Safety-factor profiles (1)

Which value of flat-top current provides a reasonable q-profile.

$$q \simeq \frac{r}{R}\frac{B_\phi}{B_\theta}$$

$$\begin{cases} B_\phi \simeq 76mT \\ B_\theta \simeq \frac{\mu_0 I}{2\pi r} \end{cases}$$

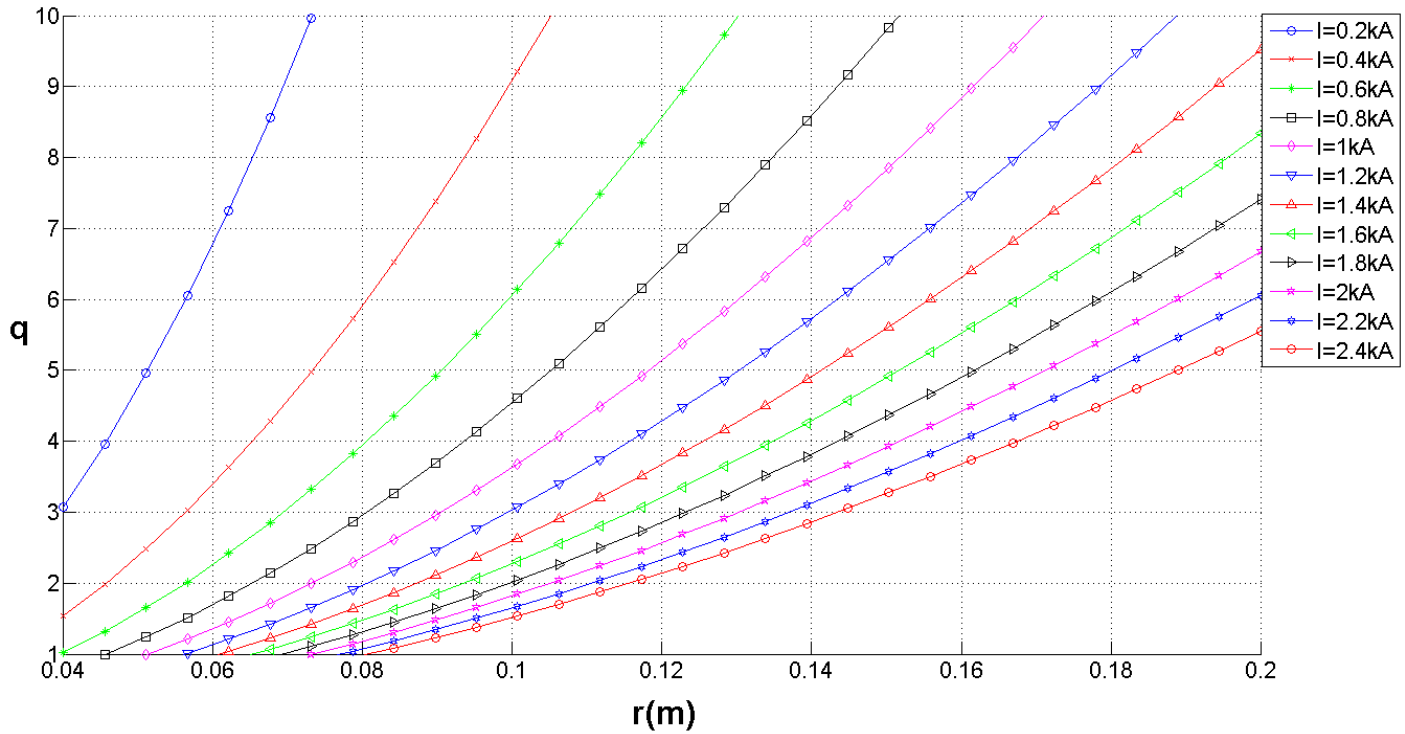

Safety-factor profiles (1)

Which value of flat-top current provides a reasonable q-profile.

$$q \simeq \frac{r}{R}\frac{B_\phi}{B_\theta}$$

$$\begin{cases} B_\phi \simeq 76mT \\ B_\theta \simeq \frac{\mu_0 I}{2\pi r} \end{cases}$$

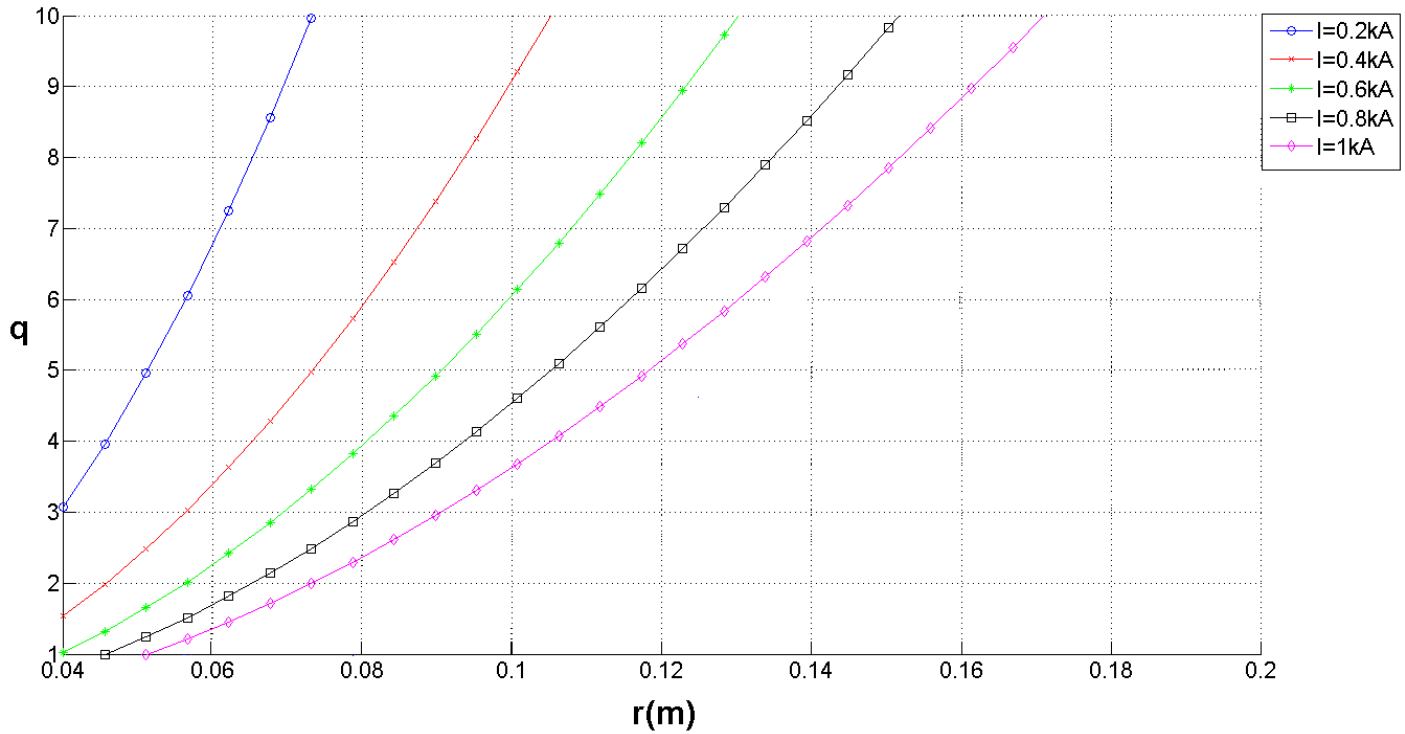

Safety factor profiles (2)

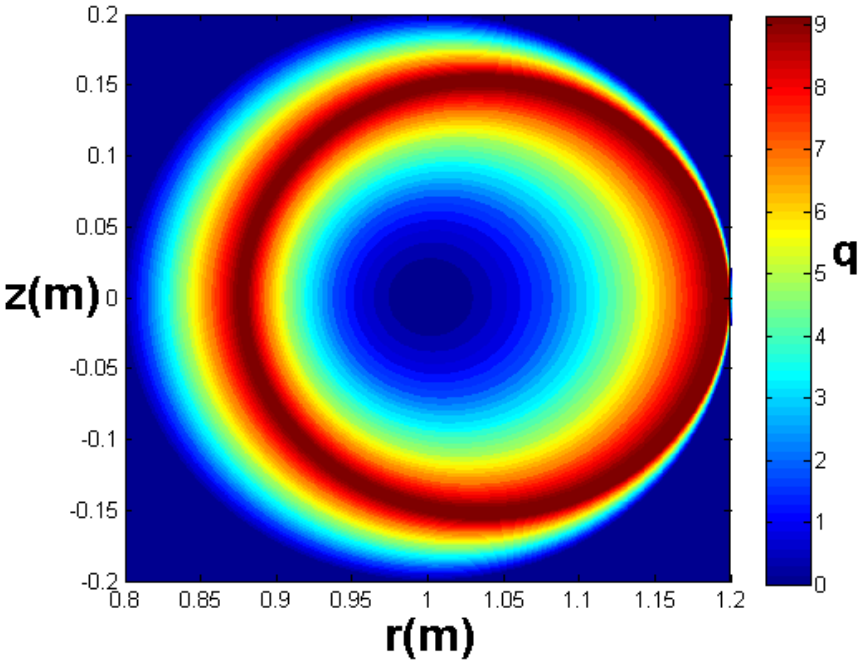

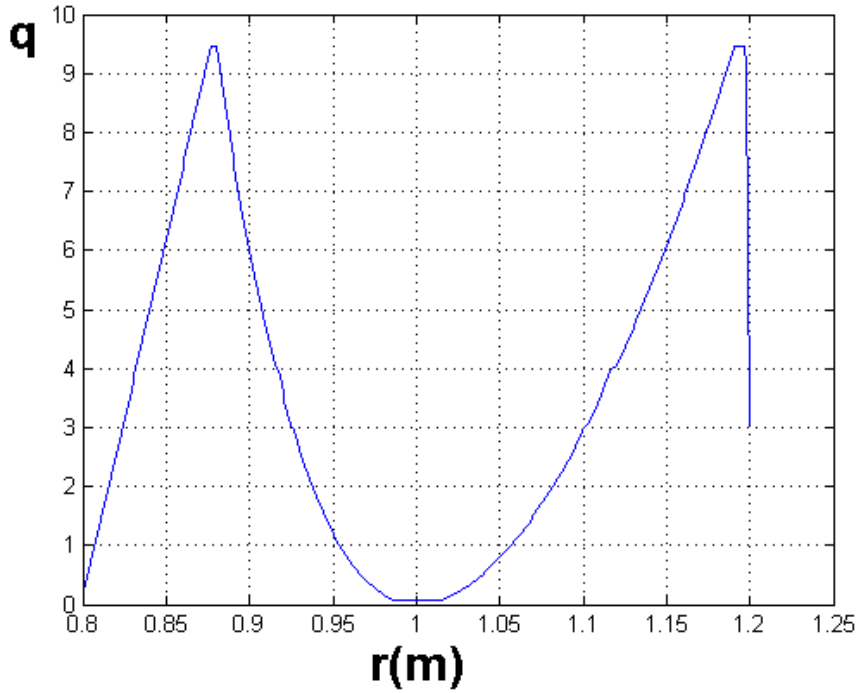

$$q = \frac{1}{2\pi} \oint \frac{1}{R} \frac{B_\phi}{B_\theta} ds$$

Heating constraint

No active cooling system assumed.

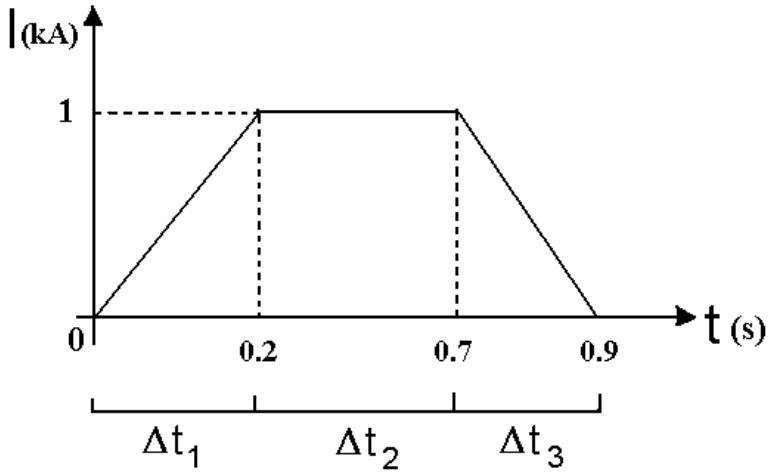

$$\Delta T \sim \frac{I_f^2}{a^4}\left(\frac{\Delta t_1 + 3\Delta t_2 + \Delta t_3}{3}\right)$$

Heating constraint

No active cooling system assumed.

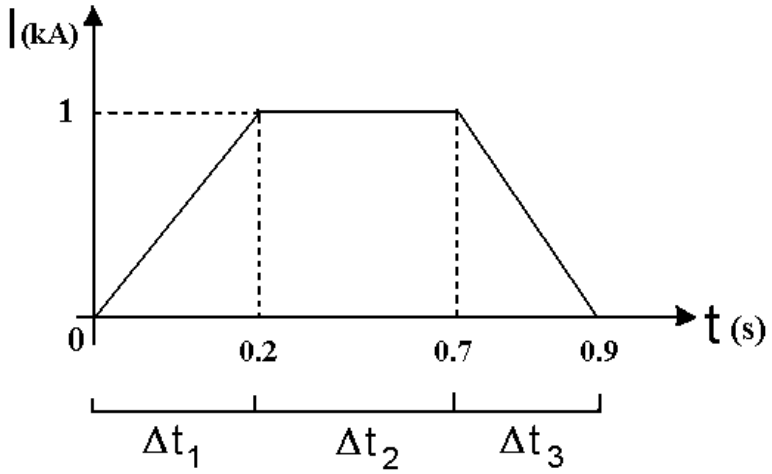

$$\Delta T \sim \frac{I_f^2}{a^4}\left(\frac{\Delta t_1 + 3\Delta t_2 + \Delta t_3}{3}\right)$$

- pure copper wire ;
- room temperature copper resistivity ;
- $a = 1cm$;
- $\Delta t_1, \Delta t_2, \Delta t_3$;

$$\Rightarrow \qquad \Delta T_{single-shot} << 1^{\circ}$$

Heating regimes

$I_f(\mathrm{kA}) \rightarrow$ / $\downarrow a(mm)$		0.4	0.6	0.8	1.0	1.2	1.4	1.6	1.8	2.0
5	$T(^\circ C)$	27°	36°	49°	67°	88°	114°	146°	182°	225°
	$\Delta L(mm)$	0.7	1.7	3.0	4.8	7.1	9.8	13.0	16.8	21.2
6	$T(^\circ C)$	23°	29°	35°	45°	56°	69°	85°	102°	123°
	$\Delta L(mm)$	0.3	0.9	1.6	2.6	3.7	5.1	6.7	8.5	10.6
7	$T(^\circ C)$	22°	25°	29°	34°	41°	49°	58°	68°	80°
	$\Delta L(mm)$	0.2	0.5	0.9	1.5	2.2	3.0	4.0	5.0	6.2
8	$T(^\circ C)$	21°	22°	26°	29°	33°	37°	44°	51°	58°
	$\Delta L(mm)$	0.1	0.2	0.6	0.9	1.4	1.9	2.5	3.2	3.9
9	$T(^\circ C)$	21°	22°	23°	26°	29°	32°	36°	41°	45°
	$\Delta L(mm)$	0.1	0.2	0.3	0.6	0.9	1.2	1.7	2.1	2.6
10	$T(^\circ C)$	20°	21°	22°	23°	26°	28°	31°	34°	38°
	$\Delta L(mm)$	0.1	0.1	0.2	0.4	0.6	0.9	1.1	1.5	1.8

Heating regimes

$I_f(\mathrm{kA}) \rightarrow$ / $\downarrow a(mm)$		0.4	0.6	0.8	1.0	1.2	1.4	1.6	1.8	2.0
5	$T(^\circ C)$	27°	36°	49°	67°	88°	114°	146°	182°	225°
	$\Delta L(mm)$	0.7	1.7	3.0	4.8	7.1	9.8	13.0	16.8	21.2
6	$T(^\circ C)$	23°	29°	35°	45°	56°	69°	85°	102°	123°
	$\Delta L(mm)$	0.3	0.9	1.6	2.6	3.7	5.1	6.7	8.5	10.6
7	$T(^\circ C)$	22°	25°	29°	34°	41°	49°	58°	68°	80°
	$\Delta L(mm)$	0.2	0.5	0.9	1.5	2.2	3.0	4.0	5.0	6.2
8	$T(^\circ C)$	21°	22°	26°	29°	33°	37°	44°	51°	58°
	$\Delta L(mm)$	0.1	0.2	0.6	0.9	1.4	1.9	2.5	3.2	3.9
9	$T(^\circ C)$	21°	22°	23°	26°	29°	32°	36°	41°	45°
	$\Delta L(mm)$	0.1	0.2	0.3	0.6	0.9	1.2	1.7	2.1	2.6
10	$T(^\circ C)$	20°	21°	22°	23°	26°	28°	31°	34°	38°
	$\Delta L(mm)$	0.1	0.1	0.2	0.4	0.6	0.9	1.1	1.5	1.8

Psitoolbox for TORPEX

Ingredients :

- TORPEX geometry.
- Poloidal flux surfaces.
- Toroidal field :
  First step $\rightarrow$ assuming $B_{\phi,0}$

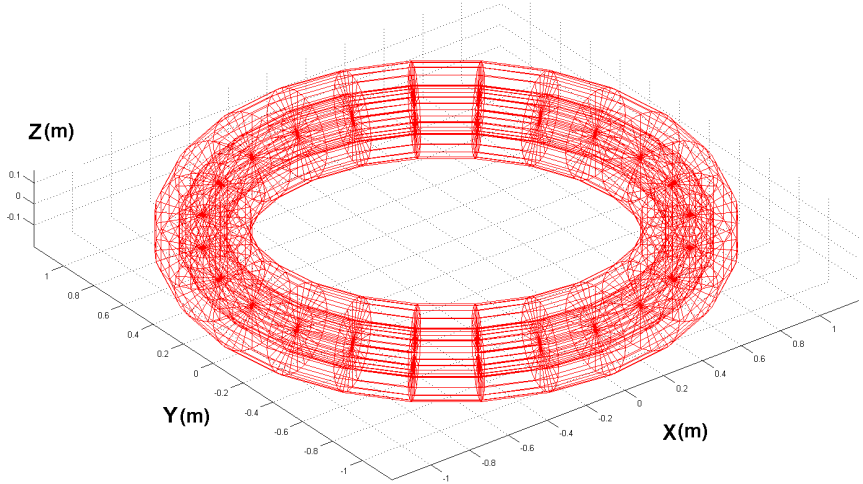

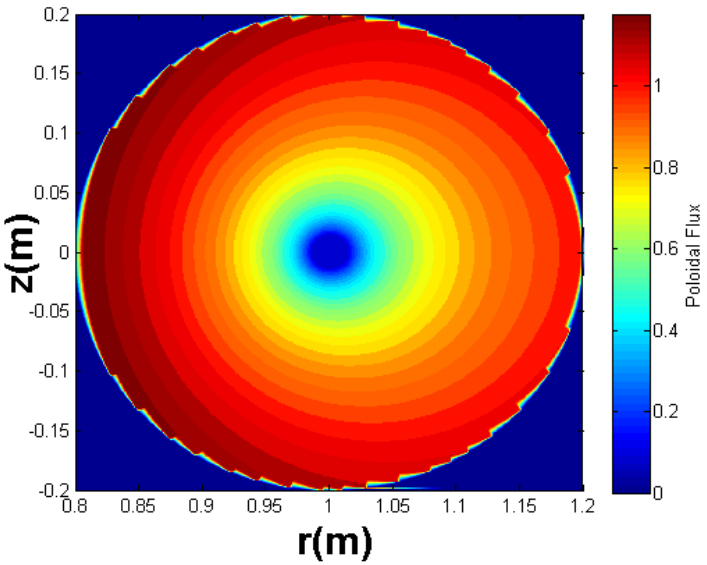

Psitoolbox for TORPEX

Ingredients :

- TORPEX geometry.
- Poloidal flux surfaces.
- Toroidal field :
  First step $\rightarrow$ assuming $B_{\phi,0}$
  Second step $\rightarrow$ inclusion of the finite number of coils (ripple).

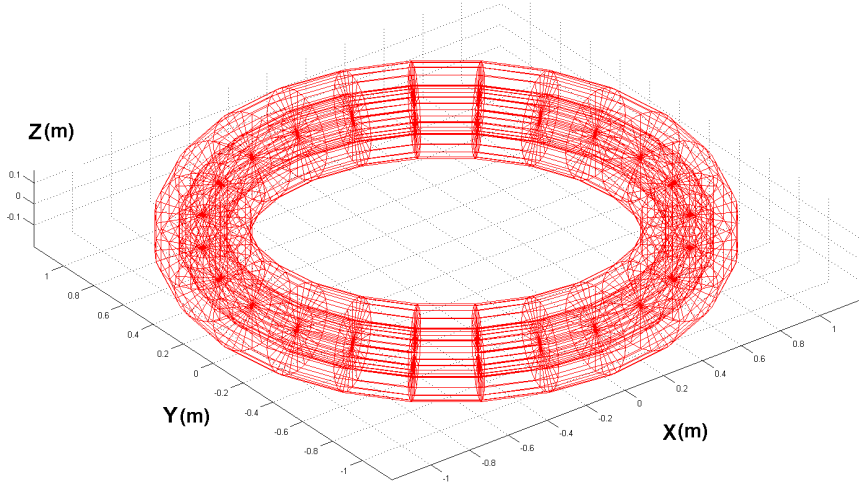

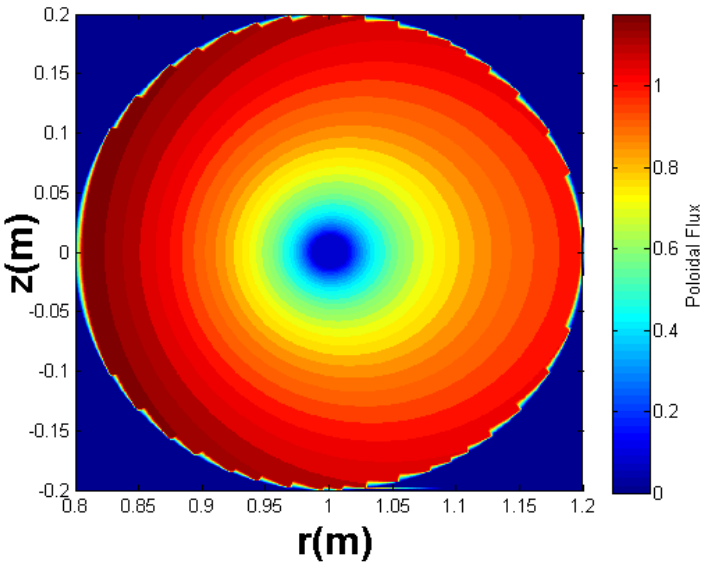

Psitoolbox for TORPEX

Ingredients :

- TORPEX geometry.
- Poloidal flux surfaces.
- Toroidal field :
  First step $\rightarrow$ assuming $B_{\phi,0}$
  Second step $\rightarrow$ inclusion of the finite number of coils (ripple).

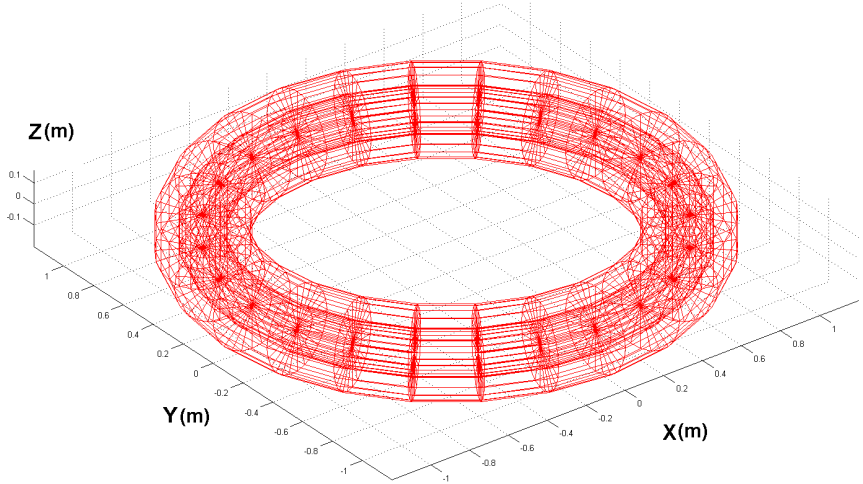

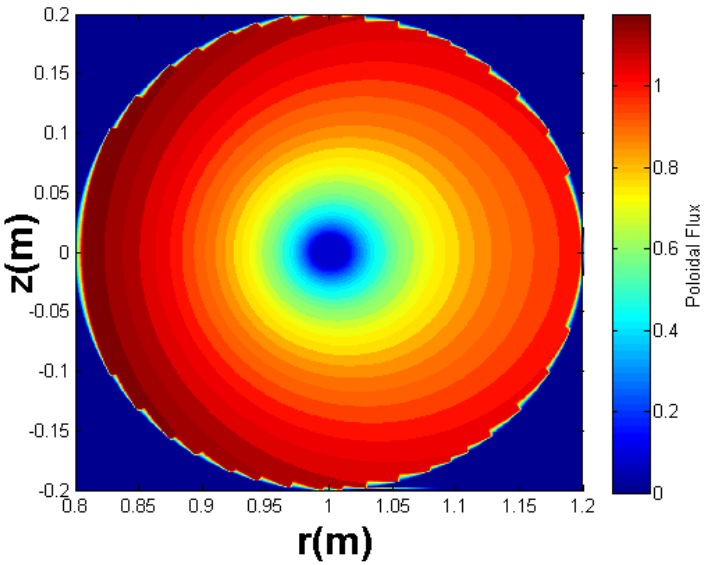

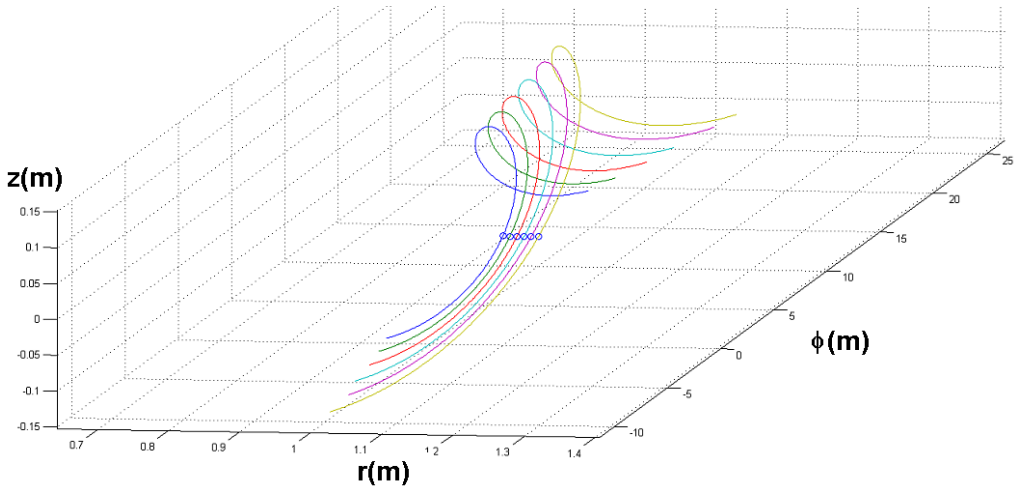

Current ripple

HEXTIP

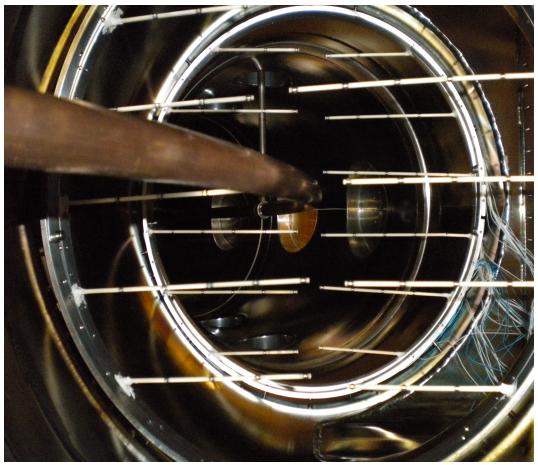

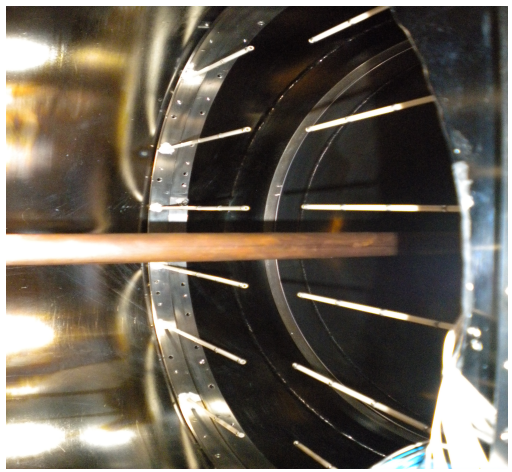

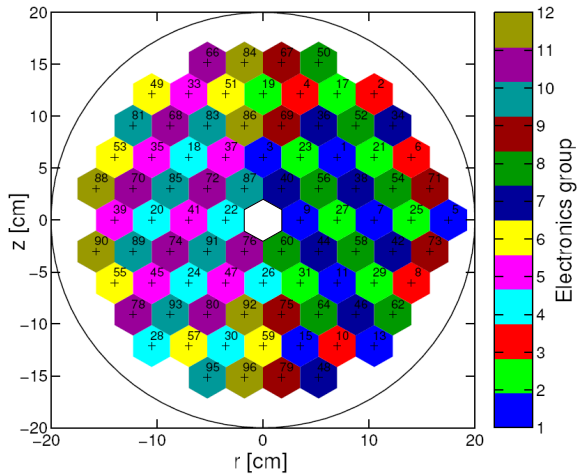

Current ripple

Langmuir probe size : $\Delta r_{Lp} \simeq 3mm$

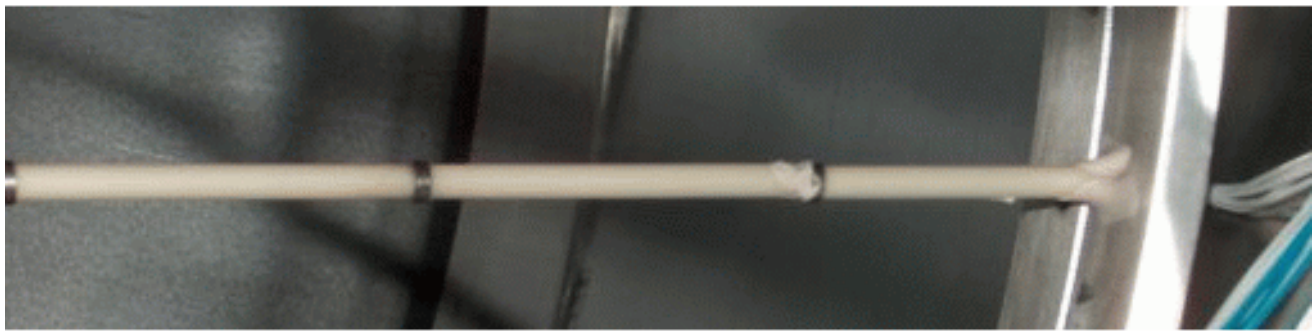

Current ripple

Langmuir probe size : $\Delta r_{Lp} \simeq 3mm$

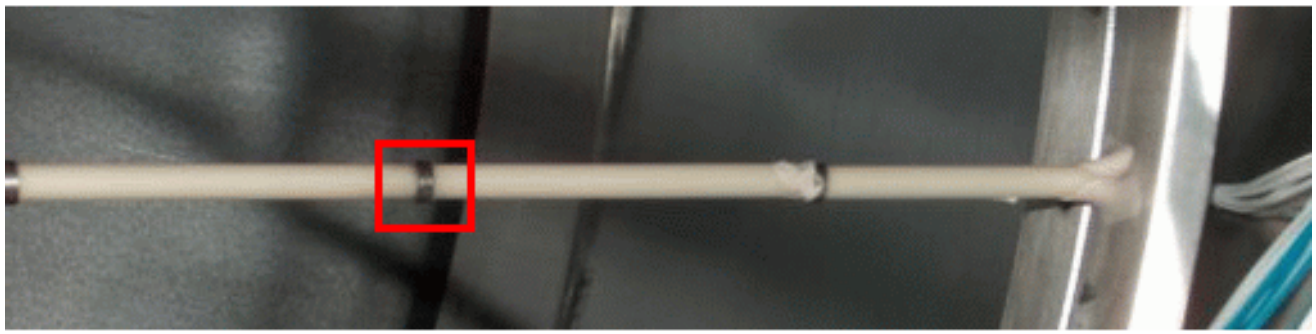

Current ripple

Langmuir probe size : $\Delta r_{Lp} \simeq 3mm \quad \Rightarrow \quad maximum \quad \Delta I_{ripple}(r_0)$.

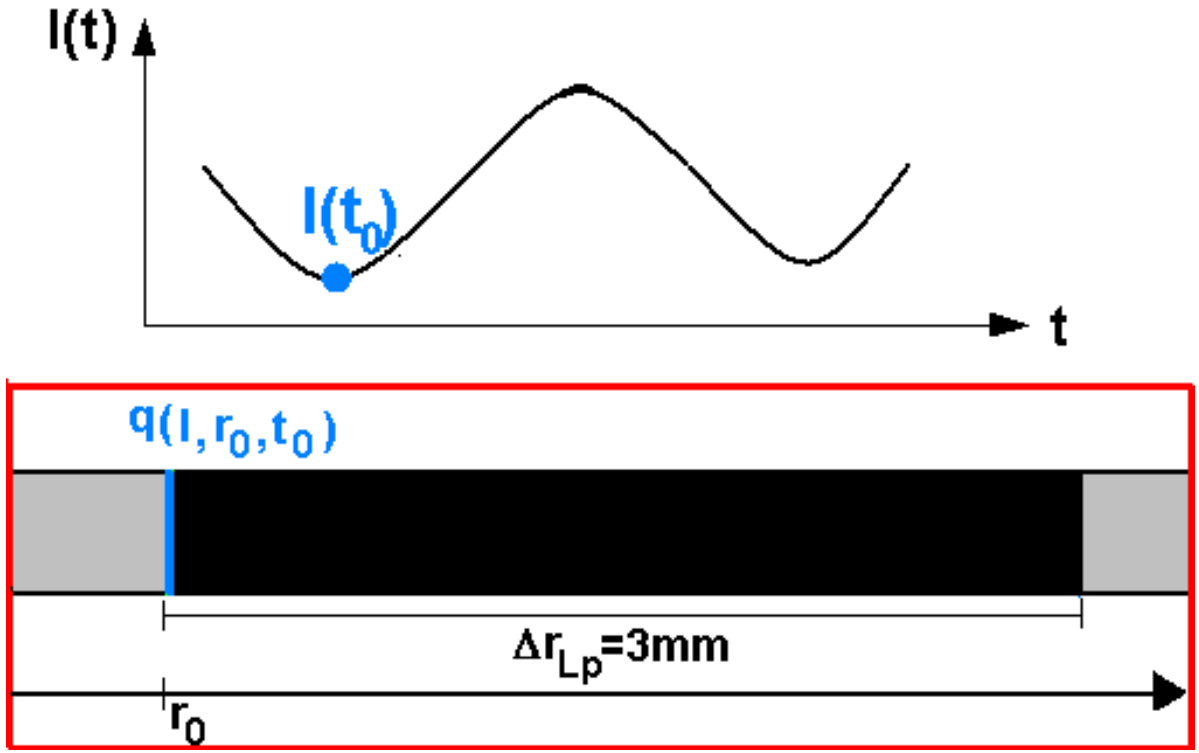

Current ripple

Langmuir probe size : $\Delta r_{Lp} \simeq 3mm \quad \Rightarrow \quad maximum \quad \Delta I_{ripple}(r_0)$.

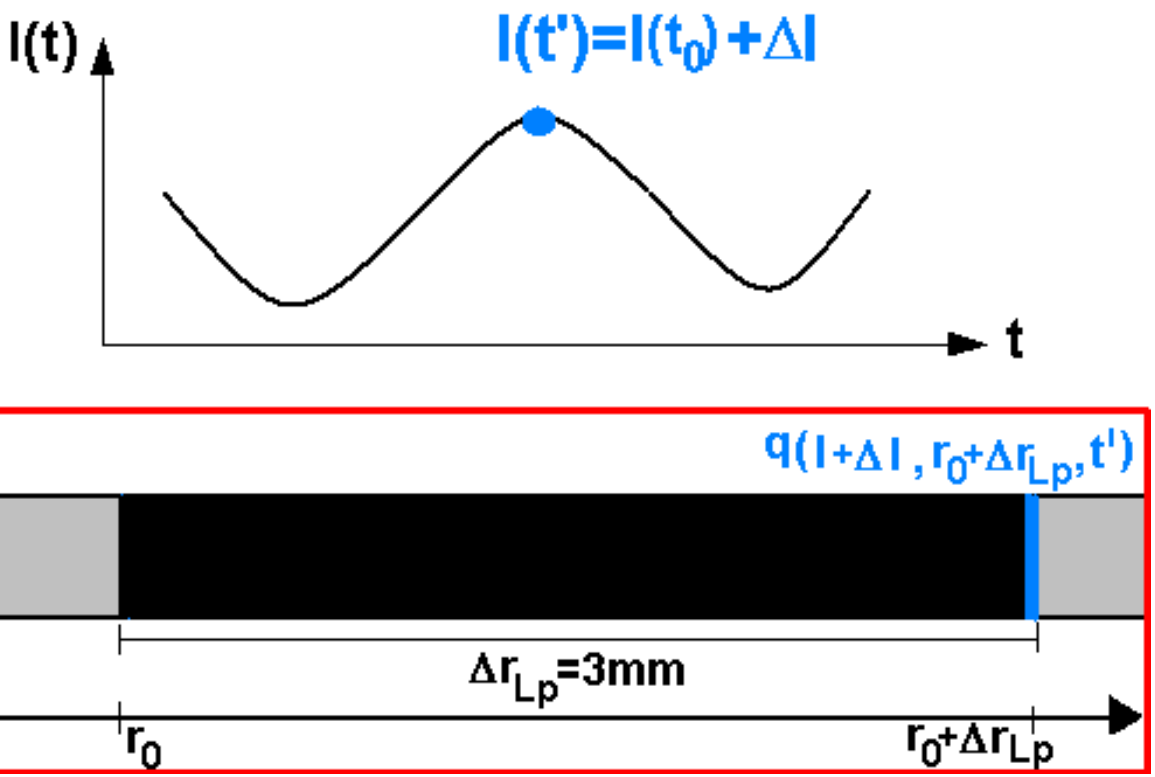

Current ripple

Langmuir probe size : $\Delta r_{Lp} \simeq 3mm \quad \Rightarrow \quad maximum \quad \Delta I_{ripple}(r_0)$.

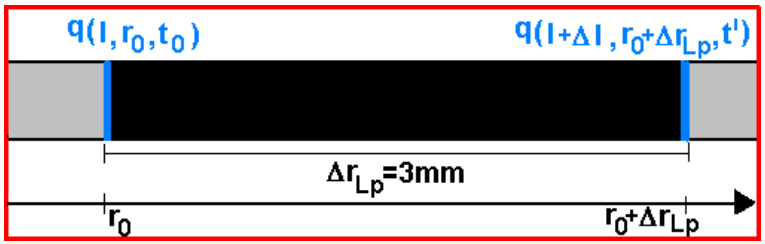

$$q = \frac{r}{R}\frac{B_T}{B_P} \underbrace{\Rightarrow}_{B_T=0.08\,T} q(r,I) \simeq 4\cdot 10^5 \frac{r^2}{I(1+r)}$$

$$q(I, r_0, t_0) = q(I + \Delta I, r_0 + \Delta r_{Lp}, t')$$

$$\frac{\Delta I}{I} = \left[\frac{(r_0+\Delta r_{Lp})^2(R+r_0)}{r_0^2(R+r_0+\Delta r_{Lp})} - 1\right]$$

The tested power supply fulfills the ripple constraint.

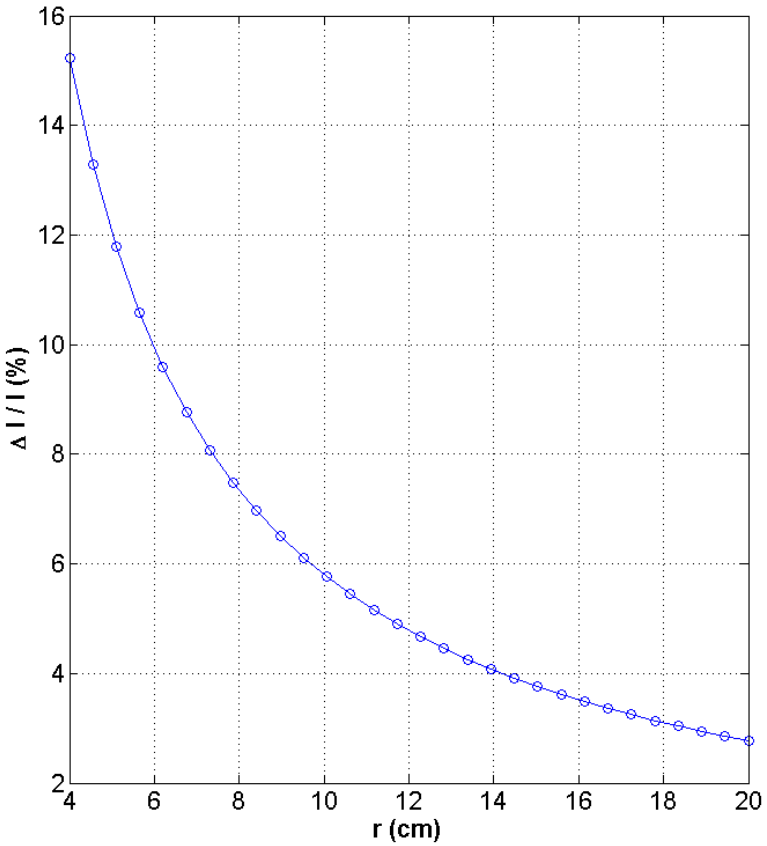

Hoop force

$$L(a,R) = R\left[\mu_0\left(\ln\frac{8R}{a} - 2\right) + \mu_0' Y\right] \simeq 6.2\times 10^{-6} H$$

$$E(R) = \frac{1}{2} I^2 L(R)$$

$$|\vec{F}_h(R)|_{R=1m} = \left|\frac{dE(R)}{dR}\right|_{R=1m} = \frac{1}{2}\mu_0 I^2\left(\ln\frac{8R}{a} + Y - 1\right)\Bigg|_{R=1m} =$$

$$= 6.28\cdot 10^{-7} I^2\left(\ln\frac{8}{a} - \frac{3}{4}\right)$$

Hoop force

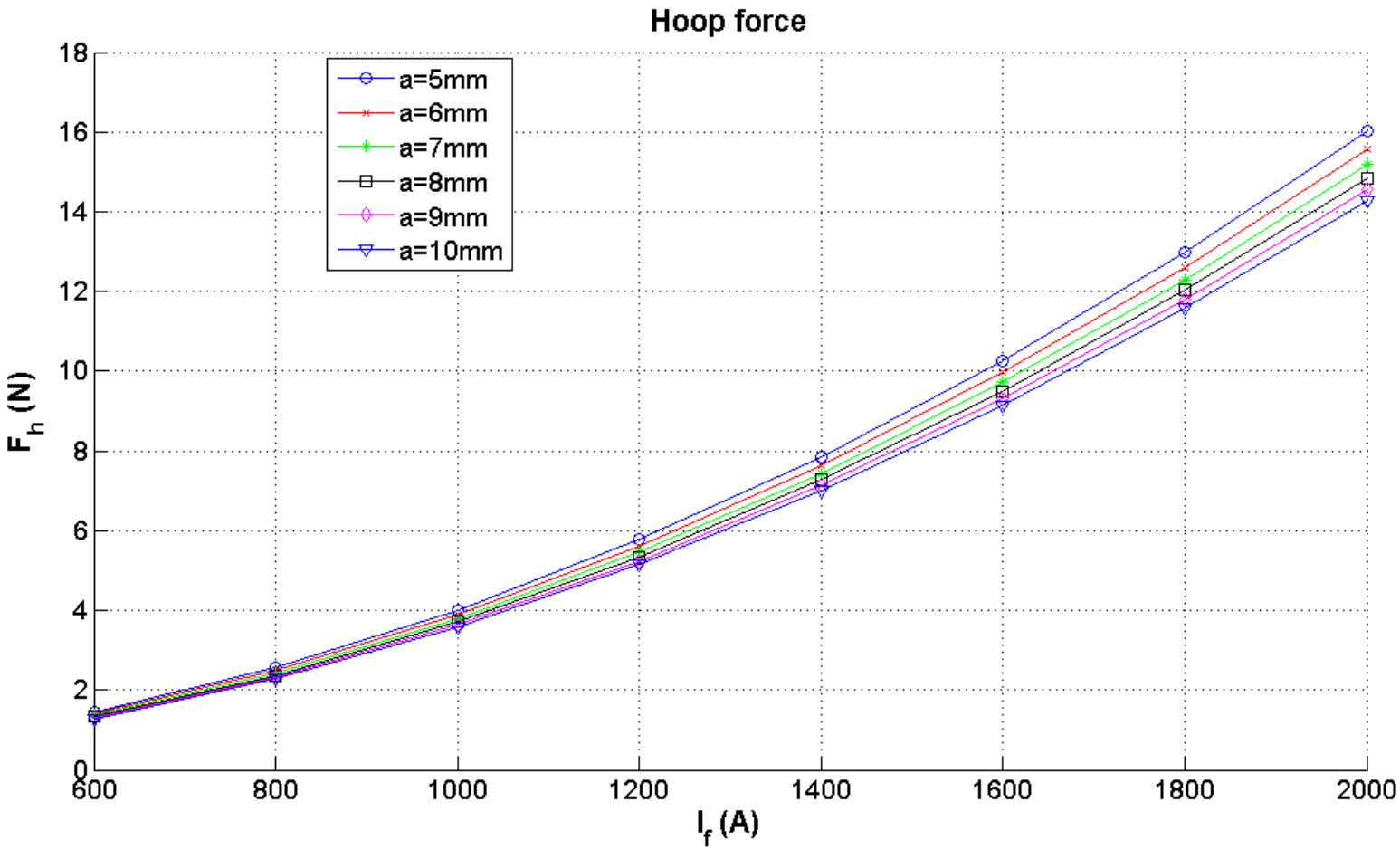
Hoop force
a=5mm
a=6mm
a=7mm
a=8mm
a=9mm
a=10mm
F_h (N)
I_f (A)
0
2
4
6
8
10
12
14
16
18
600
800
1000
1200
1400
1600
1800
2000

$\vec{I} \times \vec{B}_\phi$ force

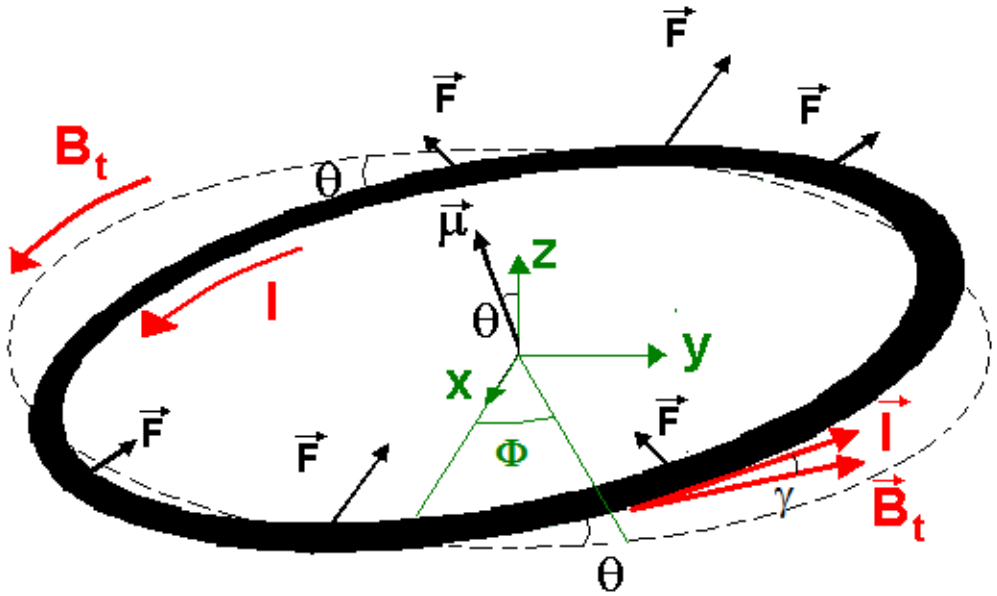

$|\vec{F}| \approx 9N$ with $\theta = 2°$ misalignment and $1kA$ of current.

$\vec{I} \times \vec{B}_\phi$ force

$$\vec{I} = \begin{pmatrix} 1 & 0 & 0 \\ 0 & \cos\theta & -\sin\theta \\ 0 & \sin\theta & \cos\theta \end{pmatrix} \cdot \begin{pmatrix} -I\sin\phi \\ I\cos\phi \\ 0 \end{pmatrix}$$

So that it follows :

$$\vec{B}_T = \begin{pmatrix} -B\sin\phi \\ B\cos\phi \\ 0 \end{pmatrix} \qquad \vec{I} = \begin{pmatrix} -I\sin\phi \\ I\cos\phi\cos\theta \\ I\cos\phi\sin\theta \end{pmatrix}$$

$$\vec{f}_L^{B_T} = \vec{I} \times \vec{B}_T = |\vec{I}||\vec{B}_T| \begin{pmatrix} -\sin\theta\cos^2\phi \\ -\sin\theta\sin\phi\cos\phi \\ \cos\theta\sin\phi\cos\phi - \cos\phi\sin\phi \end{pmatrix}$$

$$\left|F_L^{B_T}\right|_x = \left|\int_0^{2\pi} \left(f_L^{B_T}\right)_x(\theta,\phi)d\phi\right| = |\vec{I}||\vec{B}_T|\,|\Phi(\theta)| \simeq 9N$$

with a misalignment of $\theta = 2^\circ$ and a current of $I = 1kA$.

Theory group simulations

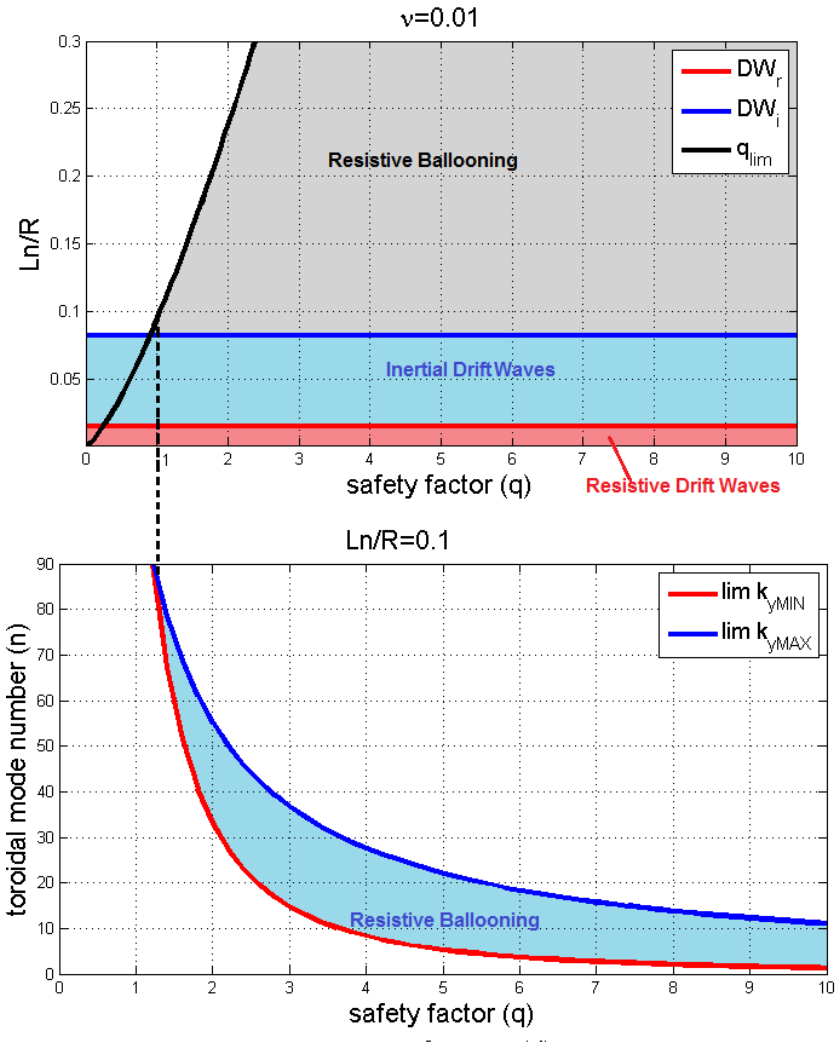

Analytical simulations performed by A.Mosetto and P. Ricci of the CRPP

Horizontal Single-Null X-point

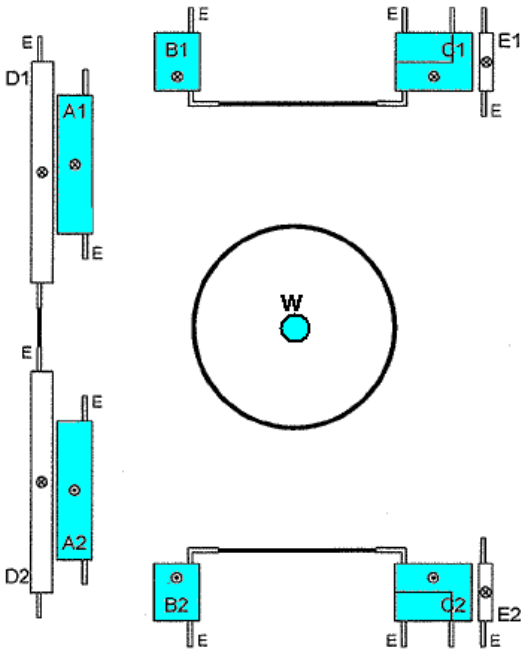

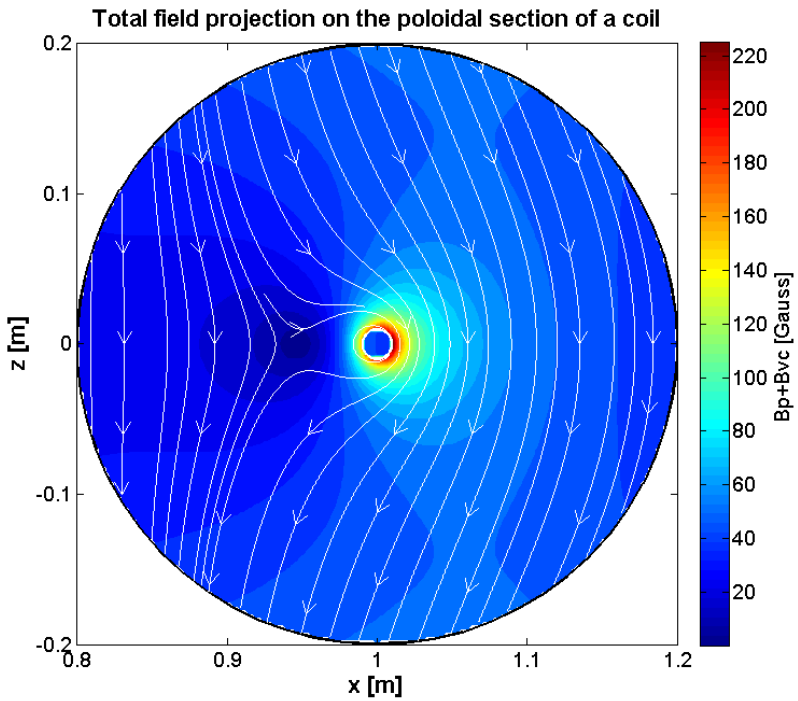

Coil	A1	A2	B1	B2	C1s	C1b	C2s	C2b	D1	D2	E1	E2	W
I $[A]$	100	100	100	100	-100	-100	-100	-100	0	0	0	0	1000

Vertical Double-Null X-point

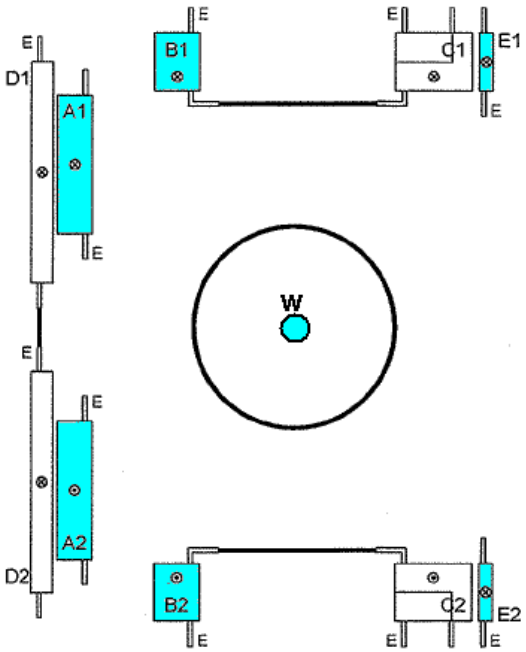

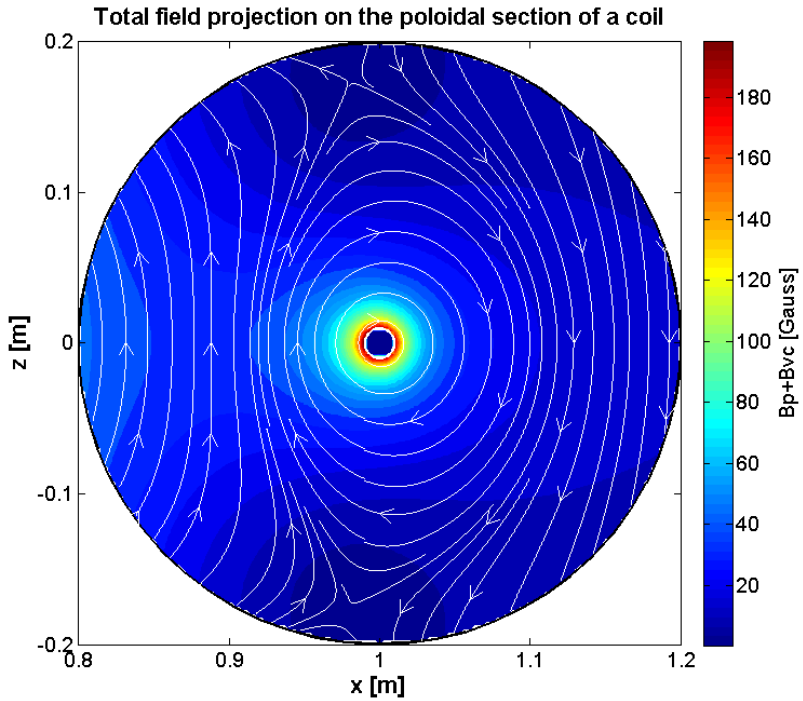

Coil	A1	A2	B1	B2	C1s	C1b	C2s	C2b	D1	D2	E1	E2	W
I $[A]$	300	300	300	300	0	0	0	0	0	0	300	300	500

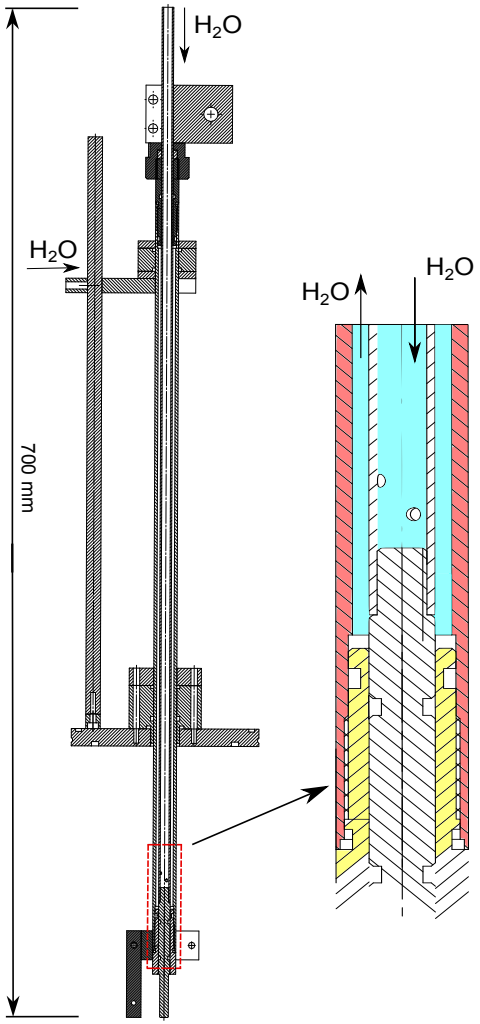
H2O
H2O
H2O
H2O
700 mm

Fourier based technique :

- Discrete Fourier Trasform (DFT)
- Spectrogram
- Power spectral density (PSD)

Statistical approach :

- Probability distribution function (PDF)
- Moments
- Correlation : cross power spectral density (CPSD)

Correlation based techniques :

- Conditional Average Sampling (CAS) $\Rightarrow$ spatio-temporal evolution of structures
- BOX-CAS $\Rightarrow$ conditionally average dynamics of n_e, T_e, V_p

Space-based technique :

- Pattern reconstruction

Two-points correlation technique

In order to compute the dispersion relation

1. Time series of two probes, divided into i windows
2. FFT to compute Fourier components from each spectrum $n^{(i)}_{1,\omega}$, $n^{(i)}_{2,\omega}$
3. Cross spectrum $\langle n^{(i)}_{1,\omega} n^{*(i)}_{2,\omega} \rangle$
4. Phase from argument $\Delta\phi = atg\left(\frac{Im\langle n^{(i)}_{1,\omega} n^{*(i)}_{2,\omega}\rangle}{Re\langle n^{(i)}_{1,\omega} n^{*(i)}_{2,\omega}\rangle}\right)$
5. $k_z(\omega) = \frac{\Delta\phi}{\Delta x}$
6. $P(k_z, \omega)$

Statistical approach to take into account the broadening of the spectrum :

$$p(k_z|\omega) = \frac{P_z(k_z,\omega)}{\sum_{k_z} P_z(k_z,\omega)} \qquad \begin{cases} \bar{k}_z(\omega) = \sum_{g-pos\ k_z} k_z p(k_z|\omega) \\ \bar{\sigma}^2_{k_z}(\omega) = \sum_{g-pos\ k_z} |k_z - \bar{k}_z(\omega)|^2 p(k_z|\omega) \end{cases}$$

Drift waves mode :

- $\vec{E} \times \vec{B}$ convection
- Can be destabilized by both resistive effects (resistive) or electron inertia (inertial, higher growth rate than resistive)
- Curvature term is no important (no q dependence)
- Shear is stabilizing

Ballooning mode (MHD toroidal mode) :

- Driven unstable from curvature
- Strongly unstable at very short wavelength
- HSF good curvature ($\vec{\kappa}$ opposite direction $\vec{\nabla} n$)
- LFS bad curvature ($\vec{\kappa}$ same direction $\vec{\nabla} n$)
- If the instability localized within bad curvature region $\rightarrow$ ballooning
- If average effect of destabilization of curvature $\rightarrow$ interchange